Brain, Behavior, and Immunity 132 (2026) 106217

Contents lists available at ScienceDirect

Brain Behavior and Immunity

journal homepage: www.elsevier.com/locate/ybrbi

Resistant starch improves Parkinson's disease symptoms through restructuring of the gut microbiome and modulating inflammation

Viacheslav A. Petrov [a,1], Sebastian Schade [b,1], Cedric C. Laczny [a,1], Jenny Hällqvist [c], Patrick May [d], Christian Jäger [e], Velma T.E. Aho [a], Oskar Hickl [d,f], Rashi Halder [g], Elisabeth Lang [b], Jordan Caussin [a], Laura A. Lebrun [a], Janine Schulz [g], Marcus Michael Unger [h], Kevin Mills [c], Brit Mollenhauer [b,i,2], Paul Wilmes [a,j,2,*]

[a] Systems Ecology group, Luxembourg Centre for Systems Biomedicine, University of Luxembourg, Esch-sur-Alzette, Luxembourg
[b] Paracelsus-Elena-Klinik, Kassel, Germany
[c] UCL Centre for Inborn Errors of Metabolism, London, United Kingdom
[d] Bioinformatics Core, Luxembourg Centre for Systems Biomedicine, University of Luxembourg, Belvaux, Luxembourg
[e] Metabolomics and Lipidomics Platform, Luxembourg Centre for Systems Biomedicine, University of Luxembourg, Belvaux, Luxembourg
[f] Department of Infection and Immunity, Luxembourg Institute of Health, Esch-sur-Alzette, Luxembourg
[g] Genomics Platform, Luxembourg Centre for Systems Biomedicine, University of Luxembourg, Belvaux, Luxembourg
[h] Department of Neurology, SHG Kliniken Sonnenberg, Saarbrücken, Germany
[i] Department of Neurology, University Medical Center Göttingen, Göttingen, Germany
[j] Department of Life Sciences and Medicine, Faculty of Science, Technology and Medicine, University of Luxembourg, Esch-sur-Alzette, Luxembourg

ARTICLE INFO

Keywords:
Parkinson's Disease
Dietary intervention
Resistant starch
Microbiome
Metagenome
Metabolome
Inflammatory proteome

ABSTRACT

Alterations in the gut microbiome and a "leaky" gut are associated with Parkinson's disease (PD), which implies the prospect of rebalancing via dietary intervention. Here, we investigate the impact of a diet rich in resistant starch on the gut microbiome through a multi-omics approach. We conducted a randomized, controlled trial with short-term and long-term phases involving 74 PD patients of three groups: conventional diet, supplementation with resistant starch, and high-fibre diet.

Our findings reveal associations between dietary patterns and changes in the gut microbiome's taxonomic composition, functional potential, metabolic activity, and host inflammatory proteome response. Resistant starch supplementation led to an increase in *Faecalibacterium* species and short-chain fatty acids alongside a reduction in opportunistic pathogens. Long-term supplementation also increased blood APOA4 and HSPA5 and reduced symptoms of PD.

Our study highlights the potential of dietary interventions to modulate the gut microbiome and improve the quality of life for PD patients.

1. Introduction

Parkinson's disease (PD) is the second most common neurodegenerative disorder. PD typically progresses slowly with early, non-motor symptoms such as constipation, loss of smell, and fatigue, developing gradually and culminating in the disruption of the extrapyramidal neuronal system. The latter results in motor complications, bradykinesia, tremor, rigidity, postural instability, and dementia in later stages (Bloem et al., 2021). One hallmark of PD-related changes in the brain is the loss of dopaminergic neurons in the substantia nigra region of the midbrain linked, for most disease phenotypes, to the accumulation of Lewy bodies – proteinaceous aggregates mostly comprised of alpha-synuclein (Bloem et al., 2021). PD-related neurodegeneration occurs not only centrally, but also in the peripheral nervous system, with the gut nervous system being involved early on (Braak et al., 2003). This is reflected by the prevalence of early gastrointestinal symptoms in the

* Corresponding author at: Luxembourg Centre for Systems Biomedicine, University of Luxembourg, Esch-sur-Alzette, Luxembourg.
E-mail address: paul.wilmes@uni.lu (P. Wilmes).
[1] shared first authors.
[2] shared last authors.

https://doi.org/10.1016/j.bbi.2025.106217
Received 16 July 2025; Received in revised form 9 November 2025; Accepted 8 December 2025
Available online 11 December 2025

preclinical stage of the disease (Warnecke et al., 2022). The full etiology of PD is still not understood, however, both genetic and environmental factors are important for disease onset and clinical course (Ben-Shlomo et al., 2024). Due to the early involvement of the gut, the role of gut-specific factors, such as the gut microbiome and nutrition, has lately gained extensive research interest in the context of PD.

The gut microbiome is altered in PD, both in drug-naive and treated patients (Scheperjans et al., 2015; Petrov et al., 2017; Hill-Burns et al., 2017; Heintz-Buschart et al., 2018; Keshavarzian et al., 2015; Aho et al., 2019; Li et al., 2019). The core changes in microbiome composition are well-replicated among different cohorts and include enrichments in specific bacterial genera, notably *Bifidobacterium*, *Lactobacillus*, *Akkermansia*, and the archaeal genus *Methanobrevibacter*, coupled to an enrichment in opportunistic pathogens and reduction of short-chain fatty acids (SCFAs) producers such as *Faecalibacterium* (Romano et al., 2021; Nishiwaki et al., 2024), which is supported by the decrease in faecal and blood levels of SCFAs seen in PD (Chen et al., 2022; Unger et al., 2016; Aho et al., 2021). This combination of changes demonstrates the development of a pro-inflammatory microbiome state, which further promotes neuroinflammation and aggravates alpha-synuclein aggregation, as recapitulated using representative animal models (Sampson et al., 2016; Kim et al., 2022).

Diet shapes the gut microbiome structure and function (Ross et al., 2024). Specifically, for PD, the quality of diet is known to affect the gut microbiome composition (Kwon et al., 2024). On the other hand, an adherence to diets rich in dietary starch has been shown to be inversely associated with PD onset and severity of clinical symptoms. According to large-scale prospective studies, a high consumption of fruits, vegetables, nuts, and tea has been linked to a decrease in the risk of PD onset (Tresserra-Rimbau et al., 2023; Gao et al., 2007). Similarly, consuming fresh vegetables, fruits, nuts, and seeds leads to an improvement of PD symptoms, while canned food, fried food, soda, and beef leads to a worsening of symptoms (Mischley et al., 2017). Thus, dietary interventions represent promising modulators to alleviate gut dysbiosis and improve the quality of life of affected individuals.

Several studies on the interaction between dietary interventions, microbiome composition, and PD clinical course have been implemented (Becker et al., 2022; Hall et al., 2023; Hegelmaier et al., 2020; Rusch et al., 2021; Bedarf et al., 2025). While these studies have demonstrated a normalisation of the gut microbiome and lessening of PD symptoms, the long-term effects and their stability have not been assessed. Here we aim to close this gap by providing a detailed analysis of the effect of short- and long-term dietary interventions on PD with an in-depth description of both the host and microbiome side. We employ metagenomic sequencing as well as metabolomics on patient-derived faecal samples to resolve the taxonomic composition and the functional potential. Inflammatory blood marker data enables the identification of differences in proteins in human circulation and linking these to taxonomic and functional microbiome features.

2. Materials and methods

2.1. Study design, participants and intervention

In a single-centre, open-label, randomised, controlled, longitudinal, interventional trial, we enrolled patients with PD by randomly applying different nutritional interventions (mixed diet group, supplement group, high-fibre group) for two weeks (short-term) followed by 48 weeks (long-term, including an 8 week wash-out phase) in a subset of the supplement group (Fig. 1).

Investigators and subjects were blinded for group allocation during baseline investigations. Subjects, aged between 40 and 85 years and diagnosed with PD in accordance with the UK Brain Bank Diagnostic Criteria (UKBBC) in Hoehn and Yahr stage 1–4 with and without motor

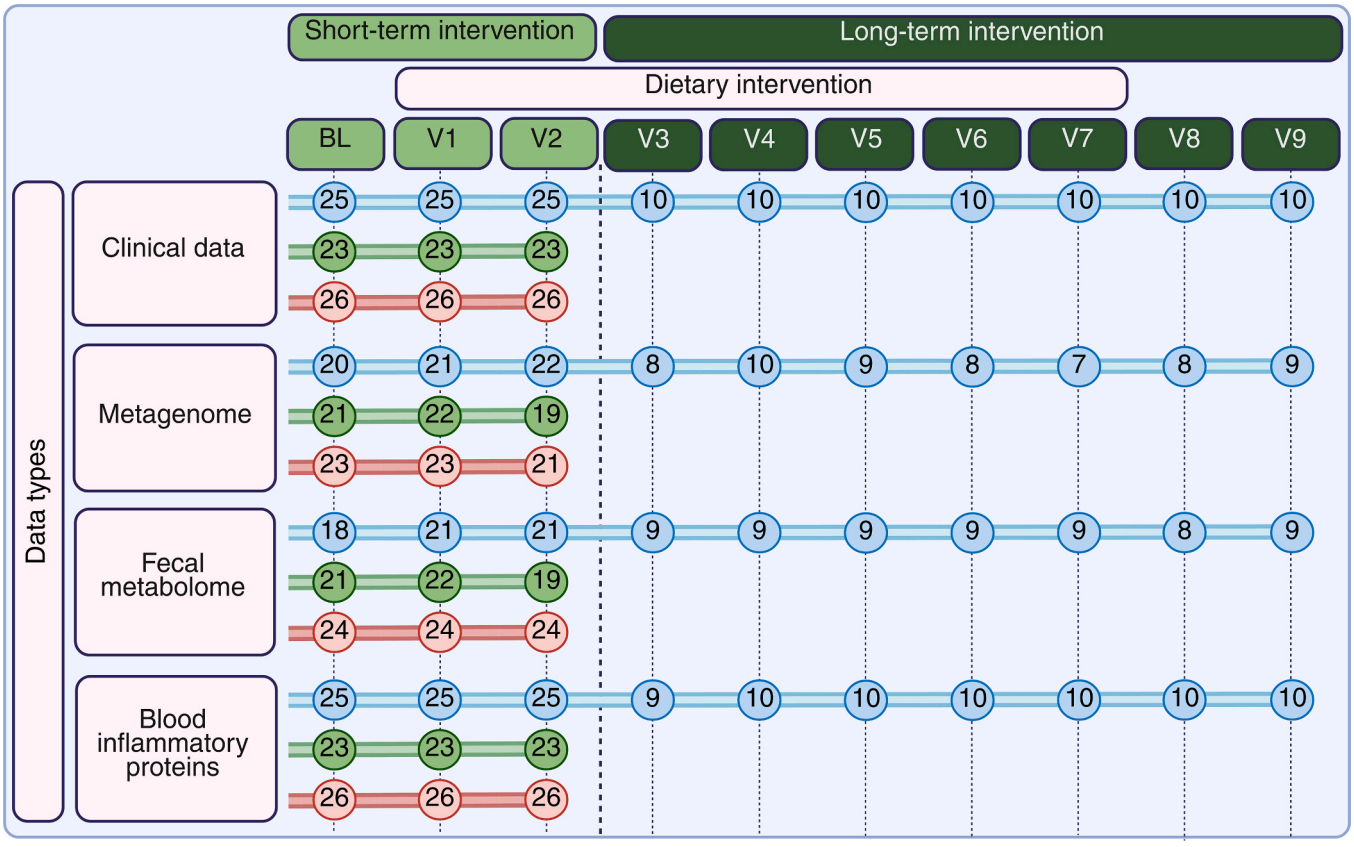

Fig. 1. Study design. The colors of the pipes represent the dietary groups: supplement group (blue), high-fibre group (green), and mixed diet group (red). The number in the circles represents the numbers of samples available for a time point. Baseline: BL, Visit: V.

fluctuations, were included after written informed consent. Subjects with known severe vascular encephalopathy or normal-pressure hydrocephalus, suspicion of atypical PD or drug-induced PD, with known intestinal pathologies (e.g. ulcerative colitis, Crohn's disease), contraindication for longitudinal blood sampling (e.g. severe anemia), use of statins, probiotic, prebiotic or antibiotic products until 4 weeks prior to study entry or patients on vegetarian/vegan diet until 4 weeks prior to study entry were excluded.

Following permuted block randomization procedures, participants were assigned to 1 of 3 treatment groups (mixed diet group, supplement group, or high-fibre group) by a computer-generated random number list using random block sizes of 6, 9, and 12. The allocation sequence was concealed by an investigator with no clinical involvement in the trial in sequentially numbered, opaque, sealed, and stapled envelopes. The envelopes were attributed to subjects consecutively according to the time of enrollment and were opened only after the enrolled participants completed all baseline investigations.

After treatment allocation, in-patient subjects in the mixed diet group received a conventional diet (ad libitum), subjects in the supplement group received 5 g resistant starch type 3 thrice daily (commercially available as SymbioIntest®) in addition to a conventional diet (ad libitum), and subjects in the high-fibre group received a high fibre/vegetarian diet. Meals were provided by the clinic's in-house kitchen for food preparation for all patients. The study was monitored by a certified dietary assistant. Subjects of the supplement group that lived close to the clinic were asked to continue in the long-term (outpatient) treatment and received 5 g resistant starch type 3 twice daily. SymbioIntest® contains resistant starch, isomaltulose, glucomannan, anticaking agent silicon dioxide, Stevia Rebaudioside, and the vitamin biotin. One sachet of SymbioIntest® stirred into a glass of non-sparkling water was drunk with the main meals.

At baseline, one week, and two weeks after treatment initiation, we collected stool and blood samples, clinical, pharmacological, and nutritional data. Faecal samples were snap-frozen immediately after defecation and stored at −80 °C until shipment for analysis. Blood samples were collected according to standardized operating and safety procedures of the Paracelsus-Elena-Klinik Kassel and stored at −80 °C until shipment for analysis. On each visit, patients were examined by a trained neurologist, and clinical data were collected using validated scales: Non-Motor Symptoms Questionnaire (NMSQ) (Chaudhuri et al., 2006), Non-Motor Symptoms Scale (NMSS) (Chaudhuri et al., 2007), Parkinson's Disease Questionnaire 39 (PDQ 39) (Jenkinson et al., 1997), Movement Disorder Society – Unified PD Rating Scale (MDS-UPDRS) (Goetz et al., 2008) parts I, II, and III. Concomitant medication was used to calculate the levodopa equivalent daily dose (LEDD) (Schade et al., 2020) Nutritional data was collected from the clinic's kitchen software "Chefs Culinar JOMOsoft" (https://www.chefsculinar.de/jomosoft-641.htm). Additionally, patients were asked to keep a separate diary of their food intake and fill in a food-frequency questionnaire.

For subjects in the long-term treatment, above mentioned investigations were repeated bimonthly for 48 weeks, of which 40 weeks were on treatment and 8 weeks post-intervention phase ("wash-out"). At these outpatient visits, returned resistant starch sachets were counted, and new sachets were distributed. For the long-term intervention, data from all participants at baseline and data from participants from the mixed diet group were used as a control.

The nutritional intervention has been defined as non-pharmacological by German authorities (Ministerium für Soziales, Gesundheit, Frauen und Familie Saarland; E 4 lfd.Nr. 98/2015) in reference to European jurisdiction (European Court of Justice, 15.11.2007 – C-319/05). The study protocol has been reviewed and approved by the local Ethics Committee (Ethik-Kommission bei der Landesärztekammer Hessen) under number FF 25/2018 and amendment 1 dated from 26.09.2018. The study has been registered in the German Clinical Trials Register (registration number DRKS00037268). The study was performed in accordance with the Declaration of Helsinki and the International Conference on Harmonization Good Clinical Practice Guidelines. All patients provided written informed consent before study participation. The incidence and severity of all adverse events (AE) were recorded according to the study protocol. The information recorded included (i) the time of the occurrence and the duration of the event; (ii) frequency of the event; (iii) severity and intensity; (iv) causality assessment; (v) outcome of the event; (vi) measures required to eliminate the consequences of the adverse event; (vii) information on the investigator registered the event. No AE occurred in this study; hence, no specific action was required.

2.2. DNA extraction and metagenomic sequencing

DNA was extracted from 150 mg of stool per sample using the DNeasy PowerLyzer PowerSoil Kit (Qiagen). The protocol of the kit was followed, with the modification that the lysis steps were performed on a Fastprep (MP Biomedicals). 750 µl of PowerBead Solution was added to the kit-provided PowerBead tube, followed by the addition of 60 µl of Solution C1. The aliquoted stool sample was added to the PowerBead tube, and bead beating was performed on a Fastprep with one cycle of 45 s at 4.0 m/sec. The resulting solution was centrifuged at 10,000 x g for 30 s, and the supernatant was transferred to a clean 2 ml Collection Tube provided in the kit. 250 µl of Solution C2 was added, vortexed for 5 s, and incubated for 5 min at 2-8° C. The tube was then centrifuged at 10,000 x g for 1 min. Up to 750 µl of the supernatant was transferred to a clean 2 ml Collection Tube provided in the kit. 200 µl of Solution C3 was added, and the tube was briefly vortexed, followed by incubation for 5 min at 2-8° C. The tube was then centrifuged at 10,000 x g for 1 min, and the supernatant was transferred to a clean 2 ml Collection Tube provided in the kit. 1200 µl of Solution C4 was added to the supernatant and vortexed for 5 s. 675 µl of the supernatant was loaded onto an MB Spin Column, centrifuged at 10,000 x g for 1 min, and the flow-through was discarded. This was repeated twice to process the entire sample. 500 µl of Solution C5 was added and centrifuged at 10,000 x g for 30 s. The flow-through was discarded, and the tube centrifuged again at 10,000 x g for 1 min. The MB Spin Column was then placed in a clean 2 ml Collection Tube provided by the kit. 100 µl of Solution C6 was added to the center of the white filter membrane and centrifuged at 10,000 x g for 30 s. The flow-through was preserved, and the MB Spin Column was discarded. DNA extraction was followed by an RNase treatment and DNA purification. RNase A (Qiagen; stock concentration 100 mg/ml) was diluted to a concentration of 20 µg/ml, added to the extracted DNA and incubated at 65 °C for 60 min. 10 % 3 M Sodium acetate (pH 5.2) and 2.5 volumes of 100 % EtOH were added. The tube was inverted to mix and kept at −20° C for 90 min. The tube was then centrifuged at maximum speed for 30 min at room temperature. The supernatant was discarded, and the remainder was washed with 70 % EtOH (400 µl). This was followed by another centrifugation at maximum speed for 5 min at room temperature. The resulting pellet was left to air-dry for 10 min and then resuspended in 40 µl H_20. DNA quality and quantity were determined using a NanoDrop spectrophotometer 1000 (Thermo Scientific) and a Qubit fluorometer (Thermo Scientific; Qubit HS DNA chip), respectively. Sample libraries were prepared using xGen DNA Lib Prep (IDT, ref. no. 10009822) according to the manufacturer's protocol. Prepared libraries were quantified using Qubit and quality controlled using a fragment analyzer. Libraries were pooled in equimolar concentration and sequenced by the Genomics platform of the Luxembourg Centre for Systems Biomedicine (LCSB) (RRID:SCR_021931) on an Illumina NextSeq2000 with a read length of 2x150bp.

2.3. Sequencing data processing and analysis

Metagenomic sequencing data were processed and assembled using the Integrated Meta-omic Pipeline (Narayanasamy et al., 2016) as follows. The reads were trimmed, quality-filtered, and then mapped against the human genome (T2TCHM13v2) to remove host

contamination. Remaining reads were assembled using MEGAHIT (Li et al., 2015) (1.2.9). Assembled contigs were annotated using Bakta (Schwengers et al., 2021), and predicted structural features were processed with Mantis (Queirós et al., 2021) for the functional annotation with KEGG (Kanehisa and Goto, 2000) (RRID:SCR_012773) and CAZy (Cantarel et al., 2009) databases. Feature quantification was done using featureCounts (Liao et al., 2014). Taxonomical annotation of the quality-filtered reads was done with Kraken2 (Wood et al., 2019) at a 0.5 confidence threshold with the GTDB (release 220) database (Parks et al., 2022). Additionally, for the prediction of microbial loads (detailed in the Statistical analysis section), microbial abundances were generated using mOTUs (Ruscheweyh et al., 2022) (3.1.0).

2.4. Faecal metabolomic analysis

The extraction and measurement of short-chain fatty acids (SCFAs), as well as the extraction and untargeted GC–MS analysis of faecal samples, were carried out as previously described by De Saedeleer et al (De Saedeleer et al., 2021). Metabolomic analysis was done by the Metabolomics platform (RRID:SCR_024769) of the LCSB. Targeted data analysis (SCFAs) was conducted using Agilent MassHunter Quantitative Analysis for GCMS software (Version 10.2, Build 10.2.733.8). Absolute quantification of target compounds was performed using external calibration curves prepared from a Volatile Free Acid Mix (Sigma-Aldrich), covering a concentration range of 10 to 4000 μmol/L. Other GC–MS chromatograms were processed using MetaboliteDetector, v3.220190704 (Hiller et al., 2009). Compounds were initially annotated by retention time and mass spectrum using an in-house mass spectral library. Internal standards were added at the same concentration to every medium sample to correct for uncontrolled sample losses and analyte degradation during metabolite extraction. The data was normalized by using the response ratio of the integrated peak area of the analyte and the integrated peak area of the internal standard.

2.5. Inflammation-related proteomic analysis

Serum samples were processed as previously described (Hällqvist et al., 2024). Specifically, serum samples were depleted from albumin and IgG using Pierce Top2 cartridges (Thermo Fisher Scientific, Waltham, Massachusetts, US) following the manufacturer's instructions. 150 μg whole protein yeast enolase (ENO1) was added to the cartridges as an internal standard to account for digestion efficiency. The depleted samples were freeze-dried before the addition of 20 μL of lysis buffer (100 mM Tris pH 7.8, 6 M urea, 2 M thiourea, and 2 % ASB-14). The samples were shaken on an orbital shaker for 60 min at 1500 rpm. To break disulphide bonds, 45 μg DTE was added and the samples incubated for 60 min. To prevent disulphide bonds from reforming, 108 μg IAA was added and the samples incubated for 45 min covered from light. 165 μL MilliQ water was added to dilute the concentration of urea and 1 μg trypsin gold (Promega, Mannheim, Germany) was added before 16 h of incubation at + 37 °C to digest the proteins into peptides. To purify the peptides, solid phase extraction was performed utilising BondElute 100 mg C18 96 well-plates (Agilent, Santa Clara, USA). The cartridges were washed with two 1 mL aliquots of 60 % ACN, and 0.1 % TFA before equilibration by two 1 mL aliquots of 0.1 % TFA. The concentration of TFA in the samples was adjusted to 0.1 %. The samples were loaded, and the flow-through was captured and reapplied. Salts were washed away from the bound peptides by two 1 mL aliquots of 0.1 % TFA. The peptides were eluted by two 250 μL aliquots of 60 % ACN, and 0.1 % TFA. Solvents were evaporated using a vacuum concentrator. Quality control (QC) samples were prepared by pooling equal amounts from a random subset of the samples. Calibration curves ranging from Lower calibrant (LLOQ) to 1 pmol/μL were constructed in blank and matrix by spiking increasing amounts of peptides into blank and QC samples. Before analysis, the samples were reconstituted in 40 μL 5 % ACN, 0.1 % FA.

Analysis was performed by targeted tandem mass spectrometry. The peptides were separated and detected on a Waters (Manchester, UK) Acquity (UPLC) system coupled to a Waters Xevo-TQ-XS triple quadrupole operating in positive ESI mode. The injection volume was 7 μL and the column was a Waters Acquity Premier Peptide BEH C18, 300Å, 1.7 μm, maintained at 40 °C. The mobile phase was A: 0.1 % formic acid in water, and B: 0.1 % formic acid in acetonitrile. The gradient elution profile was initiated with 5 % B and held for 0.25 min before linearly increasing to 40 % B over 9.75 min to elute and separate the peptides. The column was washed for 1.6 min with 85 % B before returning to the initial conditions and equilibrating for 0.4 min. The flow rate was 0.6 mL/min. Baker's yeast ENO1 was utilised to monitor digestion efficiency and as an internal standard. The amino acid sequences and instrumental parameters for the multiple reaction monitoring of each peptide can be found in Supplementary Table S19.

After acquisition, peak picking and integration were performed using TargetLynx (version 4.1, Waters) or an in-house application ("mrmIntegrate") written in Python (version 3.8, RRID:SCR_008394). mrmIntegrate is publicly available to download via the GitHub repository https://github.com/jchallqvist/mrmIntegrate. The integration method to produce areas under the curve is trapezoidal integration. The application allows for retention time alignment and simultaneous integration of the same transition for all samples. Peptide peaks were identified by the blank and matrix calibration curves. The integrated peak areas were exported to Microsoft Excel (RRID:SCR_016137) where first the ratio between quantifier and qualifier peak areas was evaluated to ensure that the correct peaks had been integrated. The quantifier area was divided by the area of the internal standard Baker's yeast ENO1 to yield a ratio used for the determination of relative concentrations. Any compound that also showed an intensity signal in the blank samples had the blank signal subtracted from the analyte peak intensity. Pooled quality control samples were additionally evaluated to assess the robustness of the run.

2.6. Statistical analysis

Statistical analysis was conducted with the R programming language version 4.4.0. Before the analysis, read-based species abundance produced by Kraken2 and functional profiles based on the KEGG and CAZy databases were filtered to retain features present in at least 30 % of samples in each group or in 50 % of samples in any one group; unidentified features were set to be zero. Faecal metabolomic data were total sample sum scaled, and inflammation-related proteome data were preprocessed as described (Section 2.5).

For the multivariate analysis, we computed distance matrices between samples based on measured features separately for each dataset. The Aitchison metric was used for taxonomic and functional microbiome profiles, and the Euclidean metric was used for the blood inflammatory proteome and faecal metabolome data. Non-metric multidimensional scaling (NMDS) was used to project the distance matrices into a two-dimensional space (monoMDS function of vegan R package (Oksanen et al., 2025) (RRID:SCR_011950). NMDS plots were manually checked for the presence of multivariate outliers, which were subsequently excluded from the downstream analysis. In total, we excluded four samples from the inflammation-related proteome data (short-term intervention) and two samples from faecal metabolomic data (longitudinal intervention). Multivariate analysis was performed with permANOVA for distance matrices (adonis2 function of vegan R package) with 9999 permutations constrained by unique patient labels and estimation of marginal effects for all terms included in the model.

Several types of technical and biological covariates were foreseen and controlled during the multivariate analysis. For all sequencing-based data, we included sequencing size factors to take into account variation in the sequencing depths between samples (with the estimateSizeFactorsForMatrix function of the DESeq2 (Love et al., 2014) R package) and predicted microbial loads (MLP (Nishijima et al., 2025) R package). For faecal metabolome data, sample batches were included as a covariate. To effectively control a wide range of potential clinical and

biological covariates, such as age, gender, body mass index (BMI), medication/LEDD, etc, we produced a linear recombination of them measured at baseline with the principal component analysis (prcomp function of stats R package, Supplementary Table S20). As a representation of covariates, we selected the first ten principal components that cumulatively explain around 55 % of the clinical data variability. For each dataset, we tested these covariates along with the dietary intervention types in a multivariate model and retained for the univariate testing only those that were significant ($p < 0.05$).

Univariate analysis was performed with Generalized Estimating Equations (geepack (Højsgaard et al., 2006) R package). The unique patient labels were used as clusters, and "ar1" was chosen as a correlation structure. Before the analysis, taxonomic and functional microbiome profiles were transformed with the centered log-ratio transformation (compositions (van den Boogaart et al., 2024) R package), and all data were mean-centered and scaled. In the case of a three-group comparison, p-values were computed with the ANOVA type II (car (Fox et al., 2024) R package), and estimated marginal means (emmeans (Lenth et al., 2025) R package) were used for the posthoc test.

Pathway enrichment analysis was conducted with the enrichKO function of the MicrobiomeProfiler R package (Yu and Chen, 2025) with standard parameters.

When applicable, p-values were adjusted for multiple testing with the Benjamini & Hochberg procedure, associations were considered significant at q-value < 0.05 after correction, and for omics-wide analysis, associations with $q < 0.1$ were considered. In addition to that, Bonferroni correction was used for the KO functional profile analysis in the longitudinal intervention. Figures were produced with BioRender and ggplot2 (Wickham et al., 2025), ggrepel (Slowikowski et al., 2024), ggpubr (Kassambara, 2023), ComplexHeatmap (Gu, 2022), and patchwork (Pedersen, 2024) R packages.

3. Results

3.1. Cohort characteristics

74 participants were included in the short-term intervention of the study (26 in the mixed diet group, 25 in the supplement group and 23 participants in the high-fibre group). Ten participants from the supplement group were enrolled in the long-term intervention (Fig. 1).

To adjust for possible clinical covariates in subsequent statistical analyses, we computed principal components (clinical PCs) based on the participants' clinical data, representing their health status at baseline of the study (detailed in Methods). Baseline characteristics of enrolled participants are summarized in Table 1. Subjects were generally well matched at baseline with no significant differences between treatment groups in age, sex, duration of the disease, LEDD, clinical PD scales, predicted gut microbial loads, or clinical PCs between the groups (Table 1).

At baseline and during each visit, participants donated stool and blood samples for the shotgun sequencing-based gut microbiome, faecal metabolome, and blood inflammatory proteome analysis. In total, 251 microbiomes, 258 faecal metabolomes, and 291 blood inflammatory proteomes were generated (Fig. 1). For each omics layer, we tested for differences in gut microbiome taxonomic composition, functional potential, and faecal metabolite and inflammatory protein levels at baseline. At baseline, no differences were identified in the studied omics features, supporting the homogeneity of the groups before the intervention (Supplementary Table S1–S6).

3.2. Results of the short-term intervention

We did not register any adverse events during the short-term intervention. As expected by the study design, individuals in the high-fibre group consumed significantly more fibre than the other groups ($p = 0.001$). To assess the influence of the short-term dietary intervention on omics features, we estimated the effect of dietary group membership, and average fibre consumption using multivariate and univariate analyses. For the multivariate analysis, we included omics-specific technical covariates as well as clinical PCs. Resistant starch consumption status was redundant with group membership and hence omitted from further analyses. The dietary pattern was significantly associated with the Kyoto Encyclopedia of Genes and Genomes (KEGG) orthologs (KO) functional potential of the microbiome, whereas the duration of the intervention correlated with the taxonomic composition and metabolic activity (Supplementary Fig. S1). Predicted microbial loads, major influencing factor for the gut microbiome (Nishijima et al., 2025), were found to be linked to both, the taxonomic and the functional composition. This measurement was therefore included along with other covariates associated with specific omics layers (Adonis2 $p < 0.05$) in the univariate model to control for confounding effects and to increase the overall statistical power.

The univariate analysis highlighted differences in taxonomic and functional composition (Figs. 2A-2G, Supplementary Table S7–S8), as well as in the faecal metabolomic profiles between the dietary groups

Table 1
Baseline characteristics of enrolled participants.

	Mixed diet group	Supplement group	High-fibre group	p
Number of participants	26	25	23	NA
Gender, female (%)	10 (38.5)	9 (36.0)	12 (52.2)	0.477
Age (mean (SD))	64.88 (9.27)	63.88 (9.08)	61.65 (8.66)	0.449
BMI (mean (SD))	26.54 (4.97)	26.96 (4.13)	26.83 (3.51)	0.939
Duration of disease, months (mean (SD))	115.04 (67.58)	76.16 (57.57)	84.87 (53.72)	0.060
LEDD (mean (SD))	885.22 (532.66)	624.31 (453.56)	723.07 (323.41)	0.119
MDS-UPDRS part I total score (mean (SD))	10.16 (6.79)	9.46 (5.62)	9.43 (5.59)	0.893
MDS-UPDRS part II total score (mean (SD))	13.52 (7.24)	12.11 (7.75)	12.05 (7.59)	0.745
MDS-UPDRS part III total score (mean (SD))	32.88 (14.22)	33.44 (11.05)	31.87 (14.98)	0.920
Hoehn and Yahr Scale (mean (SD))	2.50 (0.81)	2.28 (0.68)	2.48 (0.85)	0.550
NMSS total score (mean (SD))	53.88 (33.18)	45.08 (30.20)	44.26 (33.57)	0.507
NMSQ total score (mean (SD))	9.97 (4.91)	9.01 (5.50)	7.62 (4.23)	0.260
PDQ-39 score (mean (SD))	1.07 (0.60)	0.80 (0.56)	0.90 (0.56)	0.242
Predicted microbial loads, scaled (mean (SD))	−0.20 (0.98)	0.03 (0.87)	0.33 (0.72)	0.137
Clinical PC1 (mean (SD))	0.95 (2.96)	−0.64 (2.74)	−0.23 (2.21)	0.096
Clinical PC2 (mean (SD))	0.48 (2.22)	−0.06 (2.23)	0.05 (2.36)	0.670
Clinical PC3 (mean (SD))	−0.05 (2.33)	−0.43 (2.18)	0.56 (1.84)	0.280
Clinical PC4 (mean (SD))	−0.04 (1.96)	−0.34 (1.63)	−0.33 (1.50)	0.773
Clinical PC5 (mean (SD))	−0.44 (2.33)	−0.26 (1.97)	0.11 (1.38)	0.607
Clinical PC6 (mean (SD))	−0.05 (1.94)	−0.37 (1.86)	0.36 (1.41)	0.359
Clinical PC7 (mean (SD))	0.37 (1.86)	0.41 (1.12)	−0.22 (1.58)	0.302
Clinical PC8 (mean (SD))	−0.46 (1.86)	0.15 (1.31)	−0.07 (1.53)	0.383
Clinical PC9 (mean (SD))	0.25 (2.13)	0.03 (1.44)	−0.01 (1.18)	0.840
Clinical PC10 (mean (SD))	0.07 (1.51)	−0.34 (1.68)	−0.14 (0.83)	0.583

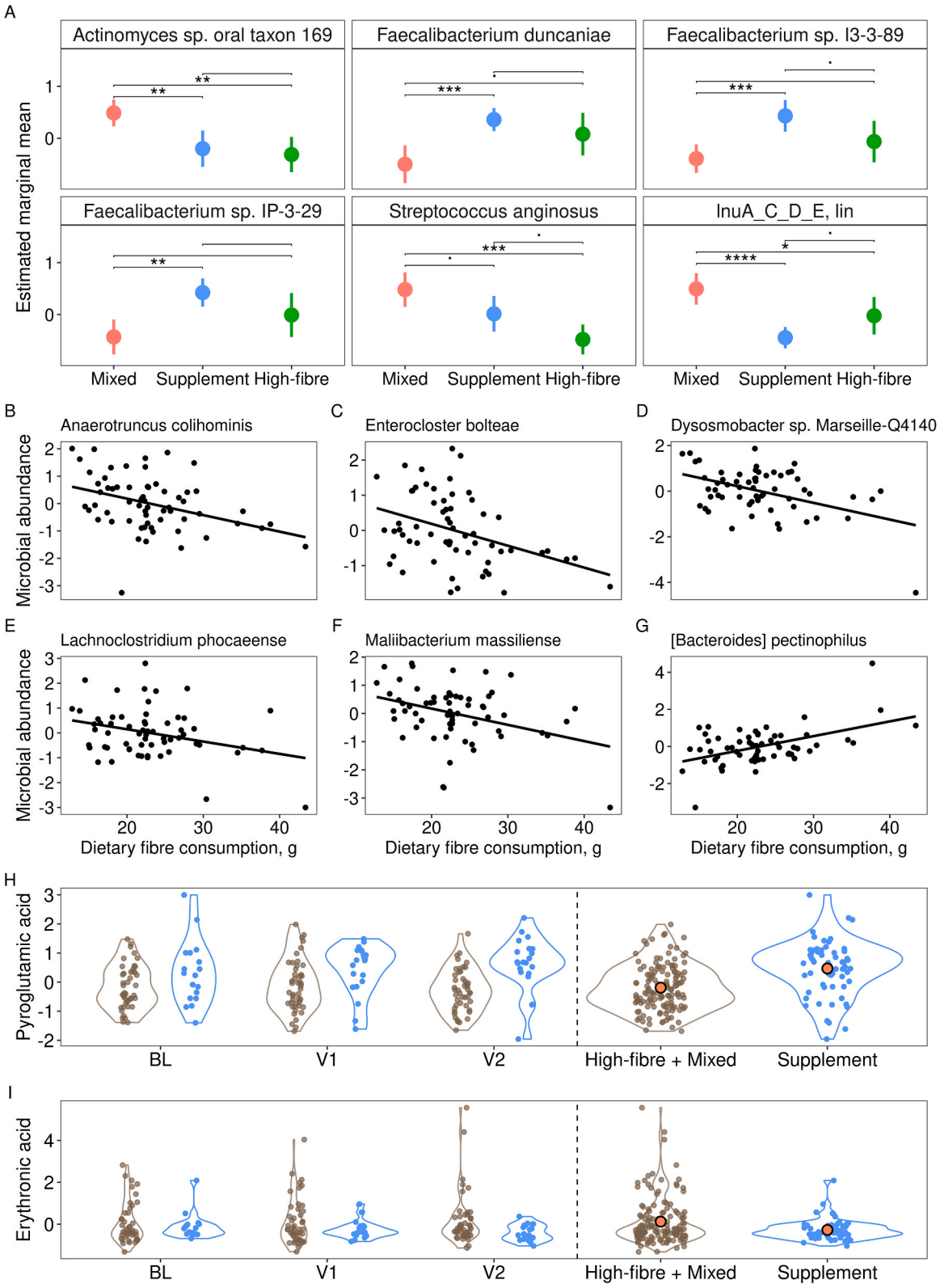

Fig. 2. Microbiome, metagenome, and metabolome differences between studied groups at the short-term intervention. (A) Differences in taxonomic composition and KEGG functional profile between the supplement (blue), high-fibre (green), and mixed diet (red) groups on the short-term intervention (Anova $q < 0.05$). Dots represent the estimated marginal means of groups, and whiskers represent standard errors. Asterisks indicate the level of significance of post-hoc comparisons (dot is $p < 0.1$, * is $p < 0.05$, ** is $p < 0.005$, *** is $p < 0.0005$, and **** is $p < 0.00005$). (B-G) Correlation between the scaled abundance of microbial species and dietary fibre consumption in grams ($q < 0.05$). (H-I) Differences in the faecal metabolome levels ($q < 0.05$) of pyroglutamic acid (H) and erythronic acid (I) at each time point (on the left) and total for the short-term intervention (on the right). For metabolites, regression residuals are plotted, orange dots represent group means.

(Figs. 2H-2I, Supplementary Table S9). Specifically, patient groups receiving either the dietary supplement or the high-fibre diet were characterized by a decrease in the abundance of antimicrobial resistance enzyme lincosamide nucleotidyltransferase A/C/D/E and *Actinomyces* sp. oral taxon 169, while *Actinomyces oris* also showed a decreasing trend (p-value = 0.006, q-value = 0.125, Supplementary Table S7). *Streptococcus anginosus* was depleted in the microbiome of individuals from the high-fibre group compared to the mixed diet group. The abundance of three *Faecalibacterium* species, namely *Faecalibacterium duncaniae*, *Faecalibacterium* sp. I3-3–89, and *Faecalibacterium* sp. IP-3–29 was increased in the supplement group compared to the mixed diet group. Dietary fibre consumption negatively correlated with the abundance of *Anaerotruncus colihominis*, *Dysosmobacter* sp. Marseille-Q4140, *Enterocloster bolteae*, *Lachnoclostridium phocaeense*, and *Maliibacterium massiliense* (Figs. 2B-2F, Supplementary Table S10). At the same time, *[Bacteroides] pectinophilus* demonstrated the opposite trend (Fig. 2G). In the faecal metabolome, dietary supplement intake was associated with an increase in pyroglutamic acid and a decrease in the levels of erythronic acid (Figs. 2H-2I, Supplementary Table S9).

3.3. Results of the long-term intervention

We did not register any adverse events during the long-term intervention. Multivariate analysis of the long-term intervention data demonstrated the correlation of the dietary supplement administration with all measured omics layers except for Carbohydrate-Active enZYmes groups (CAZy functional profile). We found the duration of the intervention to be associated with changes in the KEGG functional profile (Supplementary Fig. 2).

The KEGG functional profiles exhibited the most prominent changes in response to long-term dietary supplement administration. Specifically, 52 KEGG orthologs were significantly decreased and 191 were significantly increased after FDR adjustment, with 20 remaining significant after Bonferroni correction ($p < 0.05/5532$, Fig. 3A, Supplementary Table S11). The enrichment analysis conducted on the differentially abundant KEGG orthologs revealed increases in the following KEGG pathways in the metagenomes of individuals from the dietary supplement group: two-component system, flagellar assembly, biofilm formation, protein export, O-antigen nucleotide sugar biosynthesis, starch and sucrose metabolism, peptidoglycan biosynthesis, bacterial chemotaxis, and biosynthesis of amino acids (Fig. 3B). Pathways related to sulfur metabolism, biosynthesis of teichoic acid, terpenoid backbone and carotenoids, cationic antimicrobial peptide resistance, glycolysis, and gluconeogenesis were decreased in abundance (Fig. 3B). Within the CAZyme functional profiles, we identified a decrease in the abundance of glycoside hydrolase family 20 (GH20) and glycoside hydrolase family 33 (GH33) enzymatic groups in the metagenomes of the supplement group (Fig. 4A, Supplementary Table S12).

Dietary supplement administration was further associated with an increase in the abundance of the bacterial species *Faecalibacterium* I4-1–79, *Faecalibacterium* sp. I4-3–84, as well as the bacteriophages *Caudoviricetes* sp. and *Inoviridae* sp., whereas the abundances of the bacterial species *Olsenella uli* and *Rothia dentocariosa* were decreased (Fig. 4A, Supplementary Table S13). In the faecal metabolome of the supplement group, total SCFA levels and acetic acid increased, while erythronic acid decreased, consistent with the results of the short-term intervention (Fig. 4A, Supplementary Table S14–S15). In the inflammatory blood markers, dietary supplement intake was positively correlated with the levels of Apolipoprotein A-IV (APOA4) and heat shock protein family A member 5 (HSPA5) (Fig. 4A, Supplementary Table S16).

To assess the effect of the dietary supplement administration on the patients' condition and associated symptoms, the clinical PD scales NMSQ, NMSS, PDQ 39, MDS-UPDRS parts I, II, and III were compared before and after dietary intervention, as well as during the intervention timeline while controlling for LEDD (Fig. 4B). We identified a significant decrease in all measured clinical scales after the supplement administration (Supplementary Table S17). Additionally, the UPDRS Part III scale, which assesses the severity of motor symptoms, showed a significant decreasing trend throughout the intervention (Supplementary Table S18), while other scales exhibited non-linear dynamics over the intervention period.

3.4. Multi-omics association analysis

To further investigate inflammatory blood markers, metabolites, and microorganisms associated with both the effect of dietary intervention and PD clinical scales, we conducted an omics-wide association analysis on the whole dataset. Due to a large number of statistical tests to perform with all features from each omics layer (35,538 in total), we preselected omics features associated with the dietary intervention with $p < 0.05$ ($q < 0.05$ for the KEGG functional profiles) for the analysis, resulting in a remainder of 2,580 statistical tests overall. We focused on results with q

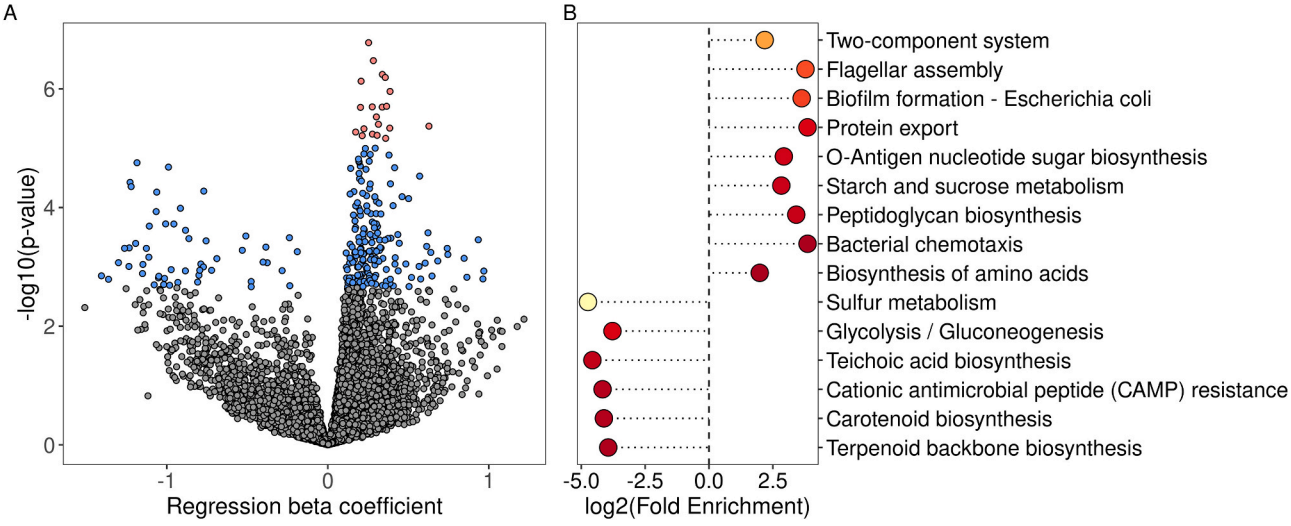

Fig. 3. Differences in KO functional profile on levels of KEGG orthologs and pathways. (A) Volcano plot of differences in KEGG orthologs between control supplement groups for the long-term intervention. The FDR-corrected statistically significant associations ($q < 0.05$) are marked in blue, the Bonferroni-corrected statistically significant associations (adj.$p < 0.05$) are marked in red, and non-significant associations ($q > 0.05$) are marked in grey. (B) Results of the pathway enrichment analysis ($q < 0.05$). The colors of the dots represent −log10 p-values (brighter colors for bigger values).

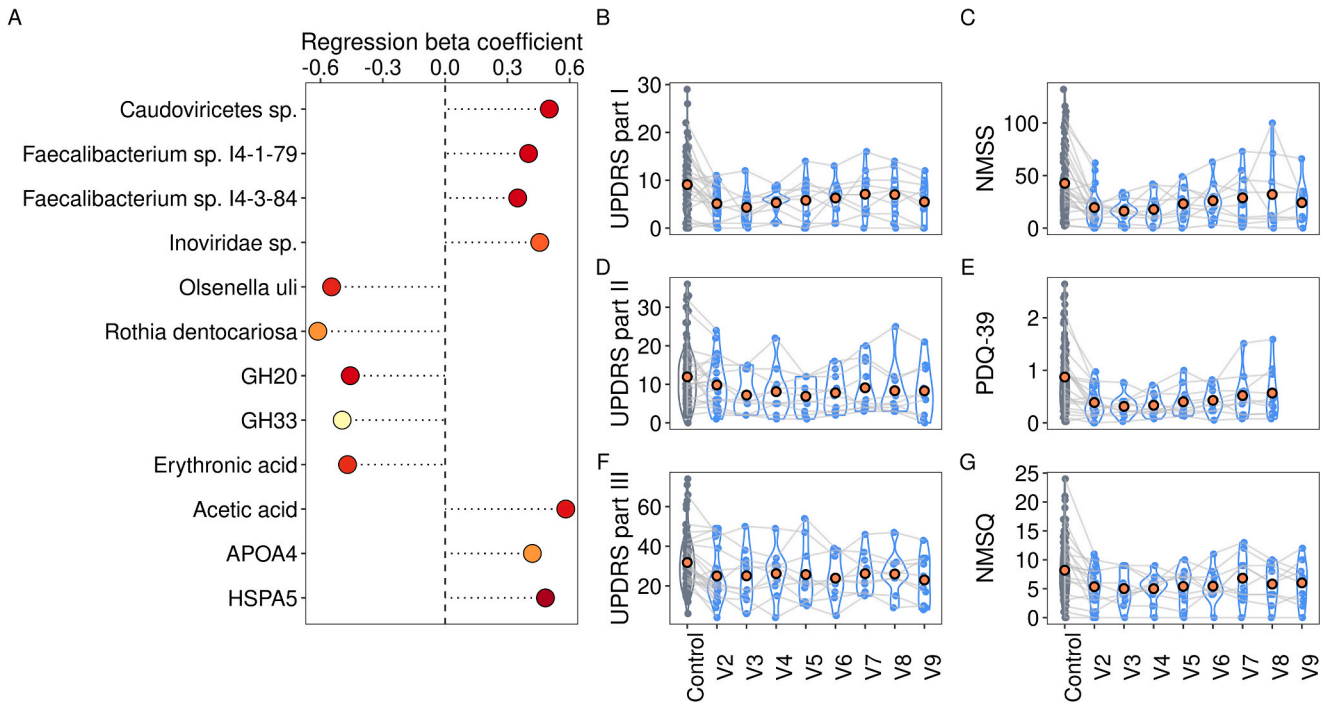

Fig. 4. Results of the long-term intervention. (A) Differences in taxonomic composition, CAZyme functional profile, faecal metabolite levels, and blood inflammatory protein levels between control supplement groups for the long-term intervention ($q < 0.05$). The color of the dots represents −log10 p-values (brighter colors for bigger values). (B-G) Results of clinical PD scales estimation for the control (in grey) and supplement (in blue) groups. Orange dots represent group means.

< 0.1, highlighting the ones with $q < 0.05$. We identified 64 associations ($q < 0.1$), with 27 of them being statistically significant ($q < 0.05$) (Fig. 5).

Several omics features correlated with improvements in PD symptoms and at the same time increased under the dietary supplement administration. We found higher blood levels of APOA4 to be associated with the improvement in non-motor symptoms of PD based on MDS-UPDRS part I, NMSS, and NMSQ scales, and quality of life measured with the PDQ 39 questionnaire. In the gut microbiome, the bacterial species *Faecalibacterium* sp. I4-3–84 and the bacteriophage species *Inoviridae* sp. were found to be associated with an improvement in participants' conditions (UPDRS part I clinical scale), whereas *Faecalibacterium* sp. I4-1–79 was found to be more abundant in individuals with improvements in the PDQ 39. In the gut metagenome, the abundances of tyramine oxidase subunit A (K25271, tynA) and CRISPR system cascade subunit CasE (K19126, casE, cse3) were associated with an improvement in PDQ 39 and, together with carbon storage regulator (K03563, csrA), the degree of motor symptoms assessed using the MDS-UPDRS part II scale. Levels of tynA, csrA, and flagellin (K02406, fliC, hag) were negatively associated with the rate and intensity of the non-motor symptoms of PD.

In addition, we identified a number of omics features correlated with the severity of PD symptoms, which simultaneously decreased during the dietary interventions. We found that the severity of non-motor symptoms in PD correlated with higher abundances in *Rothia dentocariosa* and *Enterocloster bolteae*, alongside aspartate/glutamate/glutamine transport system ATP-binding protein (K10041, peb1C/glnQ), niacin transporter (K16788, niaX), competence protein ComGA (K02243, comGA), penicillin-binding protein 1B (K03693, pbp1b), tetracycline repressor protein (K18476, tetR), amidase (K01426, E3.5.1.4, amiE), glutaminase (K23265, purQ), mevalonate kinase (K00869, MVK, mvaK1), glycoside hydrolase family 20 (GH20), and sulfite dehydrogenase subunit A (K05301, sorA). The decrease in general quality of life assessed with PDQ 39 correlated with an increase in peb1C/glnQ and amiE. The rate of PD motor symptoms (MDS-UPDRS part II) was associated with the abundances of tetR, amiE, and purQ, whereas the results of motor examination (MDS-UPDRS part III) correlated with the increase in tetR in the gut metagenome.

4. Discussion

Mounting evidence supports the role of the gut microbiome in PD pathology. Changes in diet can readily affect the gut microbiome's composition and function, and thus represent a straightforward and generally well-tolerated form of intervention. In this single-centre, randomised, controlled, longitudinal, interventional trial, we studied the effect of two nutritional interventions (high-fibre diet or dietary supplement comprised of resistant starch) compared to a conventional diet, and the impact of a longer-term supplement intervention on the individuals diagnosed with PD. During the short-term dietary intervention, we did not identify major changes in classical clinical readouts (clinical PD questionnaire, physical examination) nor the inflammatory blood biomarker profiles. However, we identified modifications of the microbiome's taxonomic structure and functional potential, as well as metabolic activity, whereby the changes are towards compositions that are typically considered to be health-promoting. Specifically, the abundances of several microorganisms and metabolites previously reported to be associated with PD changed in response to the short-term intervention. The abundances of members of the *Faecalibacterium* genus have recently been reported to be depleted in the gut microbiome of individuals with PD compared to healthy controls (Petrov et al., 2017). In the present study, the dietary supplement led to an increase in the abundance of *Faecalibacterium duncaniae*, *Faecalibacterium* sp. I3-3–89, and *Faecalibacterium* sp. IP-3–29 species in the gut microbiome. We found both the dietary supplement and high-fibre diet intake to be associated with a decrease in *Actinomyces* sp. oral taxon 169 and *Actinomyces oris* abundance in PD, while the high-fibre diet was negatively correlated with the abundance of *Anaerotruncus colihominis*. Members of these two bacterial genera, *Actinomyces* and *Anaerotruncus*, were previously found to be elevated in the gut microbiome of individuals with PD (Heintz-Buschart et al., 2018; Wallen et al., 2022; Baldini et al., 2020).

In the faecal metabolome, we identified increased pyroglutamic acid

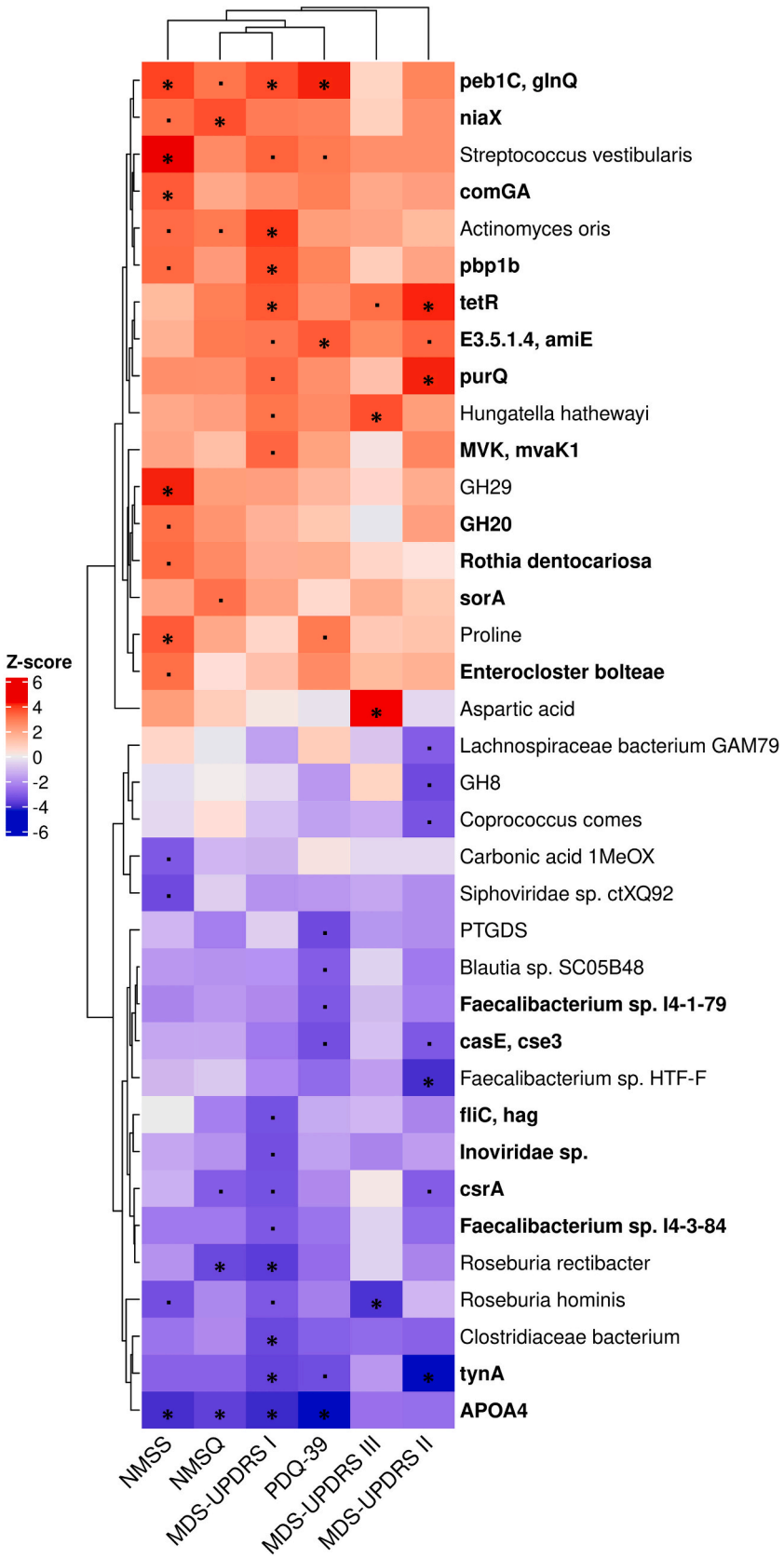

Fig. 5. Results of the multi-omics-wide association analysis on the whole dataset. The asterisk indicates the level of significance (dot is $q < 0.1$ and * is $q < 0.05$). Features with identified associations with dietary intervention are listed in bold.

levels after the administration of resistant starch supplementation. Pyroglutamic acid is an active compound of probiotic products with a number of beneficial properties, including the stimulation of GABA and acetylcholine release, which are disrupted in PD (Antonelli et al., 1984; Aiello et al., 2022). A decrease in pyroglutamic acid faecal levels has previously been reported in individuals with PD (Vascellari et al., 2020).

Mitochondrial dysfunction is one of the hallmarks of neurodegenerative diseases and is especially relevant for PD pathogenesis and disease progression (Henrich et al., 2023). We identified lower levels of erythronic acid, a marker of mitochondrial metabolism disturbance (Engelke et al., 2010) in people who received the resistant starch supplement, which could indicate improvement in mitochondrial metabolism following the intervention.

We identified additional potential health benefits of the dietary interventions. Specifically, we observed a decrease in the opportunistic pathogen *Streptococcus anginosus*, which is linked to gastrointestinal and genitourinary tract infections (Pilarczyk-Zurek et al., 2022) and *Enterocloster bolteae*, which is linked to gut dysbiosis observed in individuals with autistic spectrum disorders, multiple sclerosis, inflammatory bowel diseases, and chronic hepatitis B (Magdy Wasfy et al., 2023). A decrease in *Enterocloster bolteae* abundance in response to a Mediterranean diet in individuals with PD was shown previously (Rusch et al., 2021). In contrast, the abundance of the potential probiotic and SCFA-producing bacterium *[Bacteroides] pectinophilus* increased with increased dietary fibre intake. In the metagenome, we observed a decreased abundance of the lincosamide nucleotidyltransferase A/C/D/E ortholog, which provides resistance to lincosamide antibiotics (Brisson-Noël et al., 1988). Both interventions led to statistically significant shifts in the gut microbiome taxonomic composition.

Under long-term resistant starch supplementation, we observed, among others, an enrichment in genes related to starch and sucrose metabolism as well as an increase in total SCFA levels in the gut, including also increased levels of acetate. SCFAs provide metabolic support for colonocytes and hepatocytes (Schönfeld and Wojtczak, 2016), exhibit anti-inflammatory effects, support the maintenance of intestinal barrier integrity (Deleu et al., 2023), regulate gene expression in host cells via histone deacetylase inhibition (Chen et al., 2003), and are implicated in gut-brain axis signalling (Dalile et al., 2019). Acetate, amongst other SCFAs, has previously been reported to be decreased in individuals with PD compared to healthy individuals (Chen et al., 2022; Baert et al., 2021) Acetate is an important energy source for bacteria, including those from the *Faecalibacterium* genus (Verstraeten et al., 2024). Acetate is used in the butyrate cycle for energy production and synthesis of another SCFA, butyrate (Verstraeten et al., 2024). In addition to that, *Faecalibacterium* itself has been shown to indirectly promote SCFA production in an animal model (Zhou et al., 2021). Consistent with the link between acetate and *Faecalibacterium*, we observed a significant increase in *Faecalibacterium* sp. I4-1–79 and *Faecalibacterium* sp. I4-3–84, while *Faecalibacterium prausnitzii* and *Faecalibacterium duncaniae* showed a trend toward an increase in response to long-term resistant starch administration. These findings are in line with our results from the analyses of the short-term interventions and other reports on the effect of resistant starch on SCFA levels in the gut and blood of individuals with PD (Becker et al., 2022; Hall et al., 2023), suggesting health-beneficial changes in the gut microbiome's metabolic activity following the intervention.

The energy input received from the resistant starch supplement provides resources to support the microbiome in the large intestine. More specifically, we found enrichments in bacterial chemotaxis, two-component systems, and flagellar assembly pathways within the gut metagenome (Keegstra et al., 2022). A meta-analysis previously revealed a decrease in these pathways in the gut microbiome of individuals with PD compared to corresponding controls (Boktor et al., 2023). Our findings thus point toward the recovery of intracommunity signalling and motility during and following the intervention. Enrichments in pathways related to the synthesis of the Gram-negative bacteria cell wall (O-antigen nucleotide sugar biosynthesis, peptidoglycan biosynthesis) coupled with a decrease in the teichoic acid biosynthesis pathway, which is important for Gram-positive cell wall synthesis, suggests a community shift towards enrichments in Gram-negative bacteria. At the same time, the enrichment in genes involved in biofilm formation coupled to protein export and biosynthesis of amino acids suggests a possible motility-to-biofilm transition process and a switch towards biofilm formation (Guttenplan and Kearns, 2013; Salemi et al., 2024). On the level of individual KEGG orthologs, this shift is supported by the increase in the abundance of pilus assembly proteins (pilA, pilC, pilM). Pilins are multifunctional proteins located on the cell wall of different bacterial and archaeal species (Giltner et al., 2012) and are necessary for surface sensing and twitching motility over the surface (Persat et al., 2015). The biofilm mode of growth has been reported to be dominant for the gut microbiome and is linked to community stability (Flemming and Wuertz, 2019) and protection from intestinal damage, thus decreasing the colon permeability disrupted in PD (Nie et al., 2022; van IJzendoorn and Derkinderen, 2019). Disruption of intracommunity signalling and increase in intestinal permeability is present in a range of gut disorders, including inflammatory bowel disease (Dunleavy et al., 2025; Baldassano and Bassett, 2016), which highlights the importance of dietary-dependent microbiome modifications for general gut health.

We found that the long-term dietary intervention led to responses on the human host side. These responses include changes in the inflammatory blood proteome profiles and improvements in PD symptoms. These findings suggests lagged effects of the dietary interventions on classical clinical readouts. More specifically, we found that the levels of two blood proteins, APOA4 and HSPA5, were associated with resistant starch intake in the long-term intervention. HSPA5 is an endoplasmic reticulum chaperone involved in the unfolded protein response, which we found to be upregulated in the supplement group. Accumulating evidence shows that endoplasmic reticulum stress contributes to dopaminergic neuron vulnerability in PD and promotes alpha-synuclein aggregation (Colla et al., 2012; Mou et al., 2020). HSPA5 has been shown to be elevated in the serum of individuals with PD compared to healthy controls, reflecting an adaptive response to heightened proteostatic stress (Hällqvist et al., 2024). Several groups have reported its neuroprotective activity both *in vitro* (Jiang et al., 2016) and *in vivo* in animal models (Pazi et al., 2024; Gorbatyuk et al., 2012). Specifically, HSPA5 inhibits both microglia activation and the production of proinflammatory cytokines, tumor necrosis factor-α (TNF-α) and interleukin-6 (IL-6) (Pazi et al., 2024), markers which are typically elevated in PD (Qu et al., 2023). In contrast, its knock-down was found to increase alpha-synuclein toxicity (Salganik et al., 2015). Thus, the upregulation of this chaperone is considered a potential therapeutic target in PD (Enogieru et al., 2019). According to our results, blood HSPA5 increases in response to the dietary intervention with the resistant starch supplement which likely leads to a decrease in alpha-synuclein aggregation and toxicity and confers a beneficial effect of the diet.

APOA4 is an apolipoprotein produced in the liver and intestine and is known for its anti-inflammatory properties. APOA4 limits the secretion of proinflammatory cytokines (TNF-α, IFN-γ, and IL-4) in chronic infection models (Recalde et al., 2004). It also has a hepatoprotective effect related to acute liver injury and nonalcoholic fatty liver disease (Li et al., 2021; Liu et al., 2022) and inhibits experimental colitis (Vowinkel et al., 2004). APOA4 regulates the production of acute-phase proteins, protease inhibitors, such as SERPINA3, implicated in PD pathogenesis (Hällqvist et al., 2024) in a dose-dependent manner. More specifically, low-to-median levels of APOA4 stimulate SERPINA3 expression, while high levels of APOA4 downregulate SERPINA3 expression (Zhang et al., 2017). Beyond PD, APOA4 is also linked to Alzheimer's disease. Individuals with Alzheimer's disease show lower APOA4 expression in peripheral blood compared to healthy controls (Lin et al., 2015). In mouse models, APOA4 knockout worsens disease progression (Cui et al., 2011). In line with our results indicating associations with improvement in the NMSS and MDS-UPDRS part I scales, APOA4 was shown to be

directly associated with the results of the MoCa test in Alzheimer's disease (Kim et al., 2022), which underscores its relevance to cognitive health in neurodegenerative disorders. Currently, inflammation is recognised as an important factor in PD pathogenesis and progression (Tansey et al., 2022; Yacoubian et al., 2023). The long-term dietary intervention appears to increase APOA4 blood levels, which may mediate the health benefits by contributing to the anti-inflammatory effects of the resistant starch supplement. Taken together, these findings support a model by which dietary modulation of the gut microbiome enhances host anti-inflammatory (APOA4) and proteostatic (HSPA5) capacities. This dual action may relieve both systemic and neuronal stressors that drive PD progression. While causal links remain to be fully established, our data highlight APOA4 and HSPA5 as clinically relevant blood markers whose modulation by diet is consistent with improvements in PD symptoms.

Our results demonstrate significant improvements in the degree of motor (MDS-UPDRS parts II and III) and non-motor (MDS-UPDRS part I, NMSQ, and NMSS) symptoms as well as the quality of life (PDQ 39) of individuals with PD in response to the long-term intervention with the resistant starch supplement. Moreover, MDS-UPDRS part III scores demonstrated a significant decrease over the time of the intervention. Here, using the multi-omics-wide association analysis, we extend the identified association to a more detailed level of microbiome composition, functional potential, metabolic production, and host organism response, identifying several mechanisms of action. Specifically, bacteria from the *Faecalibacterium* genus were both affected by the dietary intervention and associated with the improvement in PD clinical scales according to our results. Notably, the lysogenic bacteriophage *Inoviridae* sp., along with the abundance of the CRISPR system cascade subunit CasE, demonstrated a similar trend. The role of bacteriophages in human health and in relation to neurodegeneration is unclear, however, it has been demonstrated that a member of *Inoviridae*, phage M13, can interact with misfolded proteins, including alpha-synuclein and amyloid beta, leading to the disruption of aggregates (Krishnan et al., 2014; Dimant et al., 2009; Dimant and Solomon, 2010). While the identified association can be a reflection of the dynamics of microbial hosts of the phage, one might speculate that the increase in the *Inoviridae* sp. itself could be linked to the improvement in participants' conditions. In addition, the abundance of tyramine oxidase subunit A ortholog was enriched after the dietary intervention and exhibited an association with an improvement in MDS-UPDRS parts I and II alongside PDQ 39 results. Tyramine oxidase subunit A is a subunit of the microbial monoaminooxidase enzyme, which catalyses the transformation of monoamines, including dopamine and tyramine, to 4-hydroxyphenylacetate (Arcos et al., 2010; Sandler et al., 1969). This compound exhibits anti-inflammatory and antioxidant effects in animal models (Liu et al., 2014; Zhao et al., 2018; An et al., 2024) and, according to Mendelian randomization analysis, mediates the microbiome effect on chronic gastritis risk (Xiang et al., 2024). The anti-inflammatory effects of this compound could mediate the health-beneficial effects of the dietary supplement.

5. Limitations

Our pilot study has several limitations. Due to the number of subjects included in this pilot study, the resulting data may not fully represent the variability of PD phenotypes and gut microbiome compositions. The long-term arm included follow-up of the intervention group only, whereas the control group was assessed at baseline but not monitored longitudinally, limiting direct comparisons between groups in terms of the longer-term effects. Detailed dietary data were not collected for the long-term intervention part. The inclusion of exercise and sleep pattern information, as well as extending the list of lifestyle factors recorded, would benefit the study and should be considered in future works.

6. Conclusions

The present randomised, controlled, longitudinal study offers a comprehensive multi-omics characterisation of the dietary interventions' impact on both the host and the gut microbiome. The results of our study demonstrate the sustainable beneficial effect of long-term resistant starch administration on both motor and non-motor symptoms of PD. The effect is mediated by the remodeling of the gut microbiome of participants, specifically an increase in the abundance of health-beneficial microorganisms such as *Faecalibacterium* and a decrease in pathogenic *Actinomyces, Rothia dentocariosa*, and *Enterocloster bolteae*. On the metagenomic level, dietary intervention improves intracommunity signalling in the gut microbiome, which is shown to be altered in PD (Boktor et al., 2023) and starch and sucrose metabolism. The metabolic readout of these changes is an increase in the faecal levels of the total SCFA and acetate – health-promoting molecules with anti-inflammatory effects known to decrease in PD and inflammatory bowel disease. From the host side, the intervention led to a decrease in erythronic acid, a marker of mitochondrial dysfunction, together with an increase in anti-inflammatory APOA4 and chaperone HSPA5, potentially mitigating PD-related neuroinflammation and alpha-synuclein toxicity. The evidence level of the findings is additionally strengthened by the randomised study design and extensive control of confounding effects.

Based on the study results, several improvements for future studies may be deduced. These include implementing a blinded, placebo-controlled design to strengthen causal inference regarding the dietary supplement, and extending the functional profiling of the microbiome beyond faecal metabolomics and metagenomics to incorporate metatranscriptomic and/or metaproteomic levels of microbial community activity. Additionally, future studies on dietary interventions in PD would benefit from stratifying participants based on polygenic risk scores, given that genetic susceptibility to PD has been shown to modulate the protective effects of plant-based diets on disease onset (Tresserra-Rimbau et al., 2023).

Data and code availability

Due to privacy restrictions, the datasets generated by this study are available upon reasonable request by contacting Paul Wilmes.

The IMP pipeline, which was used for metagenomic data analysis, is available at https://gitlab.com/uniluxembourg/lcsb/systems-ecology/imp/imp3. The R code used for statistical analyses and visualizations is available at https://gitlab.com/uniluxembourg/lcsb/systems-ecology/parkdiet.

CRediT authorship contribution statement

Viacheslav A. Petrov: Writing – original draft, Visualization, Software, Formal analysis, Data curation. **Sebastian Schade:** Writing – review & editing, Investigation, Funding acquisition, Conceptualization. **Cedric C. Laczny:** Writing – review & editing, Formal analysis. **Jenny Hällqvist:** Investigation, Formal analysis. **Patrick May:** Writing – review & editing, Investigation. **Christian Jäger:** Investigation. **Velma T. E. Aho:** Funding acquisition, Formal analysis. **Oskar Hickl:** Software, Formal analysis. **Rashi Halder:** Investigation. **Elisabeth Lang:** Investigation. **Jordan Caussin:** Investigation. **Laura A. Lebrun:** Investigation. **Janine Schulz:** Investigation. **Marcus Michael Unger:** Conceptualization. **Kevin Mills:** Investigation, Conceptualization. **Brit Mollenhauer:** Writing – review & editing, Funding acquisition, Conceptualization. **Paul Wilmes:** Writing – review & editing, Funding acquisition, Conceptualization.

Declaration of competing interest

The authors declare that they have no known competing financial

interests or personal relationships that could have appeared to influence the work reported in this paper.

Acknowledgments

This work is dedicated with deep gratitude to Dr. Sebastian Schade, whose relentless commitment, clinical expertise, and vision as a talented young clinical-scientist, Neurologist, and Movement Disorder Specialist were indispensable to its success. Sebastian's dedication to patient care and his unwavering passion for advancing our understanding of the etiology, progression, treament, and prevention of Parkinson's disease remain a cornerstone of this work, embodying the principle that science must serve humanity. Although he is no longer with us, his legacy endures through the insights and colleagues he inspired, the collaborative spirit that he embodied, and the patients he deeply cared for.

This project has received funding from the Michael J. Fox Foundation (PARKdiet MJFF-019228), the Luxembourg National Research Fund (FNR, MICROH DTU PRIDE/11823097), the Institute for Advanced Studies of the University of Luxembourg (AUDACITY grant MCI-BIOME_2019), and the European Research Council (ERC) under the European Union's Horizon 2020 research and innovation programme (grant agreement No. 863664) to P.W. Additional funding was provided by the Deutsche Forschungsgemeinschaft (DFG) Research Unit FOR2488 (INTER/DFG/19/14429377), and the FNR under the National Center of Excellence in Research on Parkinson's disease (NCER-PD, FNR11264123) to P.M. This work was also supported by a Fulbright Research Scholarship from the Commission for Educational Exchange between the United States, Belgium and Luxembourg and by the FNR under INTERMOBILITY/23/17856242 to P.W. We would like to thank Floriane Gavotto and Lucia Gallucci from the LCSB Metabolomics and Lipidomics Platform (RRID:SCR_024769) for their technical and analytical support.

Appendix A. Supplementary data

Supplementary data to this article can be found online at https://doi.org/10.1016/j.bbi.2025.106217.

Data availability

Data will be made available on request.

References

Bloem, B.R., Okun, M.S., Klein, C., 2021. Parkinson's disease. Lancet 397, 2284–2303. https://doi.org/10.1016/S0140-6736(21)00218-X.

Braak, H., Rüb, U., Gai, W.P., Del Tredici, K., 2003. Idiopathic Parkinson's disease: possible routes by which vulnerable neuronal types may be subject to neuroinvasion by an unknown pathogen. J. Neural Transm. Vienna Austria 1996 (110), 517–536. https://doi.org/10.1007/s00702-002-0808-2.

Warnecke, T., Schäfer, K.-H., Claus, I., Del Tredici, K., Jost, W.H., 2022. Gastrointestinal involvement in Parkinson's disease: pathophysiology, diagnosis, and management. NPJ Park. Dis. 8, 31. https://doi.org/10.1038/s41531-022-00295-x.

Ben-Shlomo, Y., Darweesh, S., Llibre-Guerra, J., Marras, C., San Luciano, M., Tanner, C., 2024. The epidemiology of Parkinson's disease. Lancet Lond. Engl. 403, 283–292. https://doi.org/10.1016/S0140-6736(23)01419-8.

Scheperjans, F., Aho, V., Pereira, P.A.B., Koskinen, K., Paulin, L., Pekkonen, E., Haapaniemi, E., Kaakkola, S., Eerola-Rautio, J., Pohja, M., et al., 2015. Gut microbiota are related to Parkinson's disease and clinical phenotype. Mov. Disord. off. J. Mov. Disord. Soc. 30, 350–358. https://doi.org/10.1002/mds.26069.

Petrov, V.A., Saltykova, I.V., Zhukova, I.A., Alifirova, V.M., Zhukova, N.G., Dorofeeva, Y. B., Tyakht, A.V., Kovarsky, B.A., Alekseev, D.G., Kostryukova, E.S., et al., 2017. Analysis of Gut Microbiota in patients with Parkinson's Disease. Bull. Exp. Biol. Med. 162, 734–737. https://doi.org/10.1007/s10517-017-3700-7.

Hill-Burns, E.M., Debelius, J.W., Morton, J.T., Wissemann, W.T., Lewis, M.R., Wallen, Z. D., Peddada, S.D., Factor, S.A., Molho, E., Zabetian, C.P., et al., 2017. Parkinson's Disease and PD Medications have Distinct Signatures of the Gut Microbiome. Mov. Disord. off. J. Mov. Disord. Soc. 32, 739–749. https://doi.org/10.1002/mds.26942.

Heintz-Buschart, A., Pandey, U., Wicke, T., Sixel-Döring, F., Janzen, A., Sittig-Wiegand, E., Trenkwalder, C., Oertel, W.H., Mollenhauer, B., Wilmes, P., 2018. The nasal and gut microbiome in Parkinson's disease and idiopathic rapid eye movement sleep behavior disorder. Mov. Disord. off. J. Mov. Disord. Soc. 33, 88–98. https://doi.org/10.1002/mds.27105.

Keshavarzian, A., Green, S.J., Engen, P.A., Voigt;, R.M., Naqib, A., Forsyth, C.B., Mutlu, E., Shannon, K.M., 2015. Colonic bacterial composition in Parkinson's disease. Mov. Disord. off. J. Mov. Disord. Soc. 30, 1351–1360. https://doi.org/10.1002/mds.26307.

Aho, V.T.E., Pereira, P.A.B., Voutilainen, S., Paulin, L., Pekkonen, E., Auvinen, P., Scheperjans, F., 2019. Gut microbiota in Parkinson's disease: Temporal stability and relations to disease progression. EBioMedicine 44, 691–707. https://doi.org/10.1016/j.ebiom.2019.05.064.

Li, C., Cui, L., Yang, Y., Miao, J., Zhao, X., Zhang, J., Cui, G., Zhang, Y., 2019. Gut Microbiota Differs between Parkinson's Disease patients and healthy Controls in Northeast China. Front. Mol. Neurosci. 12, 171. https://doi.org/10.3389/fnmol.2019.00171.

Romano, S., Savva, G.M., Bedarf, J.R., Charles, I.G., Hildebrand, F., Narbad, A., 2021. Meta-analysis of the Parkinson's disease gut microbiome suggests alterations linked to intestinal inflammation. Npj Park. Dis. 7, 1–13. https://doi.org/10.1038/s41531-021-00156-z.

Nishiwaki, H., Ueyama, J., Ito, M., Hamaguchi, T., Takimoto, K., Maeda, T., Kashihara, K., Tsuboi, Y., Mori, H., Kurokawa, K., et al., 2024. Meta-analysis of shotgun sequencing of gut microbiota in Parkinson's disease. Npj Park. Dis. 10, 1–11. https://doi.org/10.1038/s41531-024-00724-z.

Chen, S.-J., Chen, C.-C., Liao, H.-Y., Lin, Y.-T., Wu, Y.-W., Liou, J.-M., Wu, M.-S., Kuo, C.-H., Lin, C.-H., 2022. Association of Fecal and Plasma Levels of Short-Chain Fatty Acids with Gut Microbiota and Clinical Severity in patients with Parkinson Disease. Neurology 98. https://doi.org/10.1212/WNL.0000000000013225.

Unger, M.M., Spiegel, J., Dillmann, K.-U., Grundmann, D., Philippeit, H., Bürmann, J., Faßbender, K., Schwiertz, A., Schäfer, K.-H., 2016. Short chain fatty acids and gut microbiota differ between patients with Parkinson's disease and age-matched controls. Parkinsonism Relat. Disord. 32, 66–72. https://doi.org/10.1016/j.parkreldis.2016.08.019.

Aho, V.T.E., Houser, M.C., Pereira, P.A.B., Chang, J., Rudi, K., Paulin, L., Hertzberg, V., Auvinen, P., Tansey, M.G., Scheperjans, F., 2021. Relationships of gut microbiota, short-chain fatty acids, inflammation, and the gut barrier in Parkinson's disease. Mol. Neurodegener. 16, 6. https://doi.org/10.1186/s13024-021-00427-6.

Sampson, T.R., Debelius, J.W., Thron, T., Janssen, S., Shastri, G.G., Ilhan, Z.E., Challis, C., Schretter, C.E., Rocha, S., Gradinaru, V., et al., 2016. Gut Microbiota Regulate Motor Deficits and Neuroinflammation in a Model of Parkinson's Disease. Cell 167, 1469–1480.e12. https://doi.org/10.1016/j.cell.2016.11.018.

Kim, T.-K., Bae, E.-J., Jung, B.C., Choi, M., Shin, S.J., Park, S.J., Kim, J.T., Jung, M.K., Ulusoy, A., Song, M.-Y., et al., 2022. Inflammation promotes synucleinopathy propagation. Exp. Mol. Med. 54, 2148–2161. https://doi.org/10.1038/s12276-022-00895-w.

Ross, F.C., Patangia, D., Grimaud, G., Lavelle, A., Dempsey, E.M., Ross, R.P., Stanton, C., 2024. The interplay between diet and the gut microbiome: implications for health and disease. Nat. Rev. Microbiol. 1–16. https://doi.org/10.1038/s41579-024-01068-4.

Kwon, D., Zhang, K., Paul, K.C., Folle, A.D., Del Rosario, I., Jacobs, J.P., Keener, A.M., Bronstein, J.M., Ritz, B., 2024. Diet and the gut microbiome in patients with Parkinson's disease. NPJ Park. Dis. 10, 89. https://doi.org/10.1038/s41531-024-00681-7.

Tresserra-Rimbau, A., Thompson, A.S., Bondonno, N., Jennings, A., Kühn, T., Cassidy, A., 2023. Plant-based Dietary patterns and Parkinson's Disease: a prospective Analysis of the UK Biobank. Mov. Disord. off. J. Mov. Disord. Soc. 38, 1994–2004. https://doi.org/10.1002/mds.29580.

Gao, X., Chen, H., Fung, T.T., Logroscino, G., Schwarzschild, M.A., Hu, F.B., Ascherio, A., 2007. Prospective study of dietary pattern and risk of Parkinson disease. Am. J. Clin. Nutr. 86, 1486–1494. https://doi.org/10.1093/ajcn/86.5.1486.

Mischley, L.K., Lau, R.C., Bennett, R.D., 2017. Role of Diet and Nutritional Supplements in Parkinson's Disease Progression. Oxid. Med. Cell. Longev. 2017, 6405278. https://doi.org/10.1155/2017/6405278.

Becker, A., Schmartz, G.P., Gröger, L., Grammes, N., Galata, V., Philippeit, H., Weiland, J., Ludwig, N., Meese, E., Tierling, S., et al., 2022. Effects of Resistant Starch on Symptoms, Fecal Markers, and Gut Microbiota in Parkinson's Disease - the RESISTA-PD Trial. Genomics Proteomics Bioinformatics 20, 274–287. https://doi.org/10.1016/j.gpb.2021.08.009.

Hall, D.A., Voigt;, R.M., Cantu-Jungles, T.M., Hamaker, B., Engen, P.A., Shaikh, M., Raeisi, S., Green, S.J., Naqib, A., Forsyth, C.B., et al., 2023. An open label, non-randomized study assessing a prebiotic fiber intervention in a small cohort of Parkinson's disease participants. Nat. Commun. 14, 926. https://doi.org/10.1038/s41467-023-36497-x.

Hegelmaier, T., Lebbing, M., Duscha, A., Tomaske, L., Tönges, L., Holm, J.B., Bjørn Nielsen, H., Gatermann, S.G., Przuntek, H., Haghikia, A., 2020. Interventional Influence of the Intestinal Microbiome through Dietary intervention and Bowel Cleansing Might Improve Motor Symptoms in Parkinson's Disease. Cells 9, 376. https://doi.org/10.3390/cells9020376.

Rusch, C., Beke, M., Tucciarone, L., Nieves, C., Ukhanova, M., Tagliamonte, M.S., Mai, V., Suh, J.H., Wang, Y., Chiu, S., et al., 2021. Mediterranean Diet Adherence in people with Parkinson's Disease Reduces Constipation Symptoms and changes Fecal Microbiota after a 5-Week Single-arm pilot Study. Front. Neurol. 12, 794640. https://doi.org/10.3389/fneur.2021.794640.

Bedarf, J.R., Romano, S., Heinzmann, S.S., Duncan, A., Traka, M.H., Ng, D., Segovia-Lizano, D., Simon, M.-C., Narbad, A., Wüllner, U., et al., 2025. A prebiotic dietary pilot intervention restores faecal metabolites and may be neuroprotective in Parkinson's Disease. NPJ Park. Dis. 11, 66. https://doi.org/10.1038/s41531-025-00885-5.

Chaudhuri, K.R., Martinez-Martin, P., Schapira, A.H.V., Stocchi, F., Sethi, K., Odin, P., Brown, R.G., Koller, W., Barone, P., MacPhee, G., et al., 2006. International multicenter pilot study of the first comprehensive self-completed nonmotor symptoms questionnaire for Parkinson's disease: the NMSQuest study. Mov. Disord. off. J. Mov. Disord. Soc. 21, 916–923. https://doi.org/10.1002/mds.20844.

Chaudhuri, K.R., Martinez-Martin, P., Brown, R.G., Sethi, K., Stocchi, F., Odin, P., Ondo, W., Abe, K., Macphee, G., Macmahon, D., et al., 2007. The metric properties of a novel non-motor symptoms scale for Parkinson's disease: results from an international pilot study. Mov. Disord. off. J. Mov. Disord. Soc. 22, 1901–1911. https://doi.org/10.1002/mds.21596.

Jenkinson, C., Fitzpatrick, R., Peto, V., Greenhall, R., Hyman, N., 1997. The Parkinson's Disease Questionnaire (PDQ-39): development and validation of a Parkinson's disease summary index score. Age Ageing 26, 353–357. https://doi.org/10.1093/ageing/26.5.353.

Goetz, C.G., Tilley, B.C., Shaftman, S.R., Stebbins, G.T., Fahn, S., Martinez-Martin, P., Poewe, W., Sampaio, C., Stern, M.B., Dodel, R., et al., 2008. Movement Disorder Society-sponsored revision of the Unified Parkinson's Disease Rating Scale (MDS-UPDRS): scale presentation and clinimetric testing results. Mov. Disord. off. J. Mov. Disord. Soc. 23, 2129–2170. https://doi.org/10.1002/mds.22340.

Schade, S., Mollenhauer, B., Trenkwalder, C., 2020. Levodopa Equivalent Dose Conversion Factors: an Updated Proposal Including Opicapone and Safinamide. Mov. Disord. Clin. Pract. 7, 343–345. https://doi.org/10.1002/mdc3.12921.

Narayanasamy, S., Jarosz, Y., Muller, E.E.L., Heintz-Buschart, A., Herold, M., Kaysen, A., Laczny, C.C., Pinel, N., May, P., Wilmes, P., 2016. IMP: a pipeline for reproducible reference-independent integrated metagenomic and metatranscriptomic analyses. Genome Biol. 17, 260. https://doi.org/10.1186/s13059-016-1116-8.

Li, D., Liu, C.-M., Luo, R., Sadakane, K., Lam, T.-W., 2015. MEGAHIT: an ultra-fast single-node solution for large and complex metagenomics assembly via succinct de Bruijn graph. Bioinforma. Oxf. Engl. 31, 1674–1676. https://doi.org/10.1093/bioinformatics/btv033.

Schwengers, O., Jelonek, L., Dieckmann, M.A., Beyvers, S., Blom, J., Goesmann, A., 2021. Bakta: rapid and standardized annotation of bacterial genomes via alignment-free sequence identification. Microb. Genomics 7, 000685. https://doi.org/10.1099/mgen.0.000685.

Queirós, P., Delogu, F., Hickl, O., May, P., Wilmes, P., 2021. Mantis: flexible and consensus-driven genome annotation. GigaScience 10, giab042. https://doi.org/10.1093/gigascience/giab042.

Kanehisa, M., Goto, S., 2000. KEGG: Kyoto encyclopedia of genes and genomes. Nucleic Acids Res. 28, 27–30. https://doi.org/10.1093/nar/28.1.27.

Cantarel, B.L., Coutinho, P.M., Rancurel, C., Bernard, T., Lombard, V., Henrissat, B., 2009. The Carbohydrate-active EnZymes database (CAZy): an expert resource for Glycogenomics. Nucleic Acids Res. 37. https://doi.org/10.1093/nar/gkn663.

Liao, Y., Smyth, G.K., Shi, W., 2014. featureCounts: an efficient general purpose program for assigning sequence reads to genomic features. Bioinforma. Oxf. Engl. 30, 923–930. https://doi.org/10.1093/bioinformatics/btt656.

Wood, D.E., Lu, J., Langmead, B., 2019. Improved metagenomic analysis with Kraken 2. Genome Biol. 20, 257. https://doi.org/10.1186/s13059-019-1891-0.

Parks, D.H., Chuvochina, M., Rinke, C., Mussig, A.J., Chaumeil, P.-A., Hugenholtz, P., 2022. GTDB: an ongoing census of bacterial and archaeal diversity through a phylogenetically consistent, rank normalized and complete genome-based taxonomy. Nucleic Acids Res. 50. https://doi.org/10.1093/nar/gkab776.

Ruscheweyh, H.-J., Milanese, A., Paoli, L., Karcher, N., Clayssen, Q., Keller, M.I., Wirbel, J., Bork, P., Mende, D.R., Zeller, G., et al., 2022. Cultivation-independent genomes greatly expand taxonomic-profiling capabilities of mOTUs across various environments. Microbiome 10, 212. https://doi.org/10.1186/s40168-022-01410-z.

De Saedeleer, B., Malabirade, A., Ramiro-Garcia, J., Habier, J., Trezzi, J.-P., Peters, S.L., Daujeumont, A., Halder, R., Jäger, C., Busi, S.B., et al., 2021. Systematic characterization of human gut microbiome-secreted molecules by integrated multi-omics. ISME Commun. 1, 1–6. https://doi.org/10.1038/s43705-021-00078-0.

Hiller, K., Hangebrauk, J., Jäger, C., Spura, J., Schreiber, K., Schomburg, D., 2009. MetaboliteDetector: comprehensive analysis tool for targeted and nontargeted GC/MS based metabolome analysis. Anal. Chem. 81, 3429–3439. https://doi.org/10.1021/ac802689c.

Hällqvist, J., Bartl, M., Dakna, M., Schade, S., Garagnani, P., Bacalini, M.-G., Pirazzini, C., Bhatia, K., Schreglmann, S., Xylaki, M., et al., 2024. Plasma proteomics identify biomarkers predicting Parkinson's disease up to 7 years before symptom onset. Nat. Commun. 15, 4759. https://doi.org/10.1038/s41467-024-48961-3.

Oksanen, J., Simpson, G.L., Blanchet, F.G., Kindt, R., Legendre, P., Minchin, P.R., O'Hara, R.B., Solymos, P., Stevens, M.H.H., Szoecs, E., et al. (2025). vegan: Community Ecology Package. Version 2.6-10.

Love, M.I., Huber, W., Anders, S., 2014. Moderated estimation of fold change and dispersion for RNA-seq data with DESeq2. Genome Biol. 15, 550. https://doi.org/10.1186/s13059-014-0550-8.

Nishijima, S., Stankevic, E., Aasmets, O., Schmidt, T.S.B., Nagata, N., Keller, M.I., Ferretti, P., Juel, H.B., Fullam, A., Robbani, S.M., et al., 2025. Fecal microbial load is a major determinant of gut microbiome variation and a confounder for disease associations. Cell 188, 222–236.e15. https://doi.org/10.1016/j.cell.2024.10.022.

Højsgaard, S., Halekoh, U., Yan, J., 2006. The R Package geepack for Generalized estimating Equations. J. Stat. Softw. 15, 1–11. https://doi.org/10.18637/jss.v015.i02.

Boogaart, K.G. van den, Tolosana-Delgado, R., and Bren, M. (2024). compositions: Compositional Data Analysis. Version 2.0-8.

Fox, J., Weisberg, S., Price, B., Adler, D., Bates, D., Baud-Bovy, G., Bolker, B., Ellison, S., Firth, D., Friendly, M., et al. (2024). car: Companion to Applied Regression. Version 3.1-3.

Lenth, R.V., Banfai, B., Bolker, B., Buerkner, P., Giné-Vázquez, I., Herve, M., Jung, M., Love, J., Miguez, F., Piaskowski, J., et al., 2025. emmeans: estimated Marginal Means, aka Least-Squares Means. Version 1 (11), 1.

Yu, G., and Chen, M. MicrobiomeProfiler: An R/shiny package for microbiome functional enrichment analysis. *R package version 1.14.0*. https://doi.org/10.18129/B9.bioc.MicrobiomeProfiler.

Wickham, H., Chang, W., Henry, L., Pedersen, T.L., Takahashi, K., Wilke, C., Woo, K., Yutani, H., Dunnington, D., van den Brand, T., et al., 2025. ggplot2: create Elegant Data Visualisations using the Grammar of Graphics. Version 3 (5), 2.

Slowikowski, K., Schep, A., Hughes, S., Dang, T.K., Lukauskas, S., Irisson, J.-O., Kamvar, Z.N., Ryan, T., Christophe, D., Hiroaki, Y., et al., 2024. ggrepel: Automatically Position Non-Overlapping Text Labels with "ggplot2. Version (9), 6.

Kassambara, A., 2023. ggpubr: "ggplot2" based Publication Ready Plots. Version (6).

Gu, Z., 2022. Complex Heatmap Visualization. Imeta 1, e43.

Pedersen, T.L., 2024. patchwork: the composer of Plots. Version 1 (3).

Wallen, Z.D., Demirkan, A., Twa, G., Cohen, G., Dean, M.N., Standaert, D.G., Sampson, T. R., Payami, H., 2022. Metagenomics of Parkinson's disease implicates the gut microbiome in multiple disease mechanisms. Nat. Commun. 13, 6958. https://doi.org/10.1038/s41467-022-34667-x.

Baldini, F., Hertel, J., Sandt, E., Thinnes, C.C., Neuberger-Castillo, L., Pavelka, L., Betsou, F., Krüger, R., Thiele, I., and NCER-PD Consortium, 2020. Parkinson's disease-associated alterations of the gut microbiome predict disease-relevant changes in metabolic functions. BMC Biol. 18, 62. https://doi.org/10.1186/s12915-020-00775-7.

Antonelli, T., Carlà, V., Lambertini, L., Moroni, F., Bianchi, C., 1984. Pyroglutamic acid administration modifies the electrocorticogram and increases the release of acetylcholine and GABA from the guinea-pig cerebral cortex. Pharmacol. Res. Commun. 16, 189–197. https://doi.org/10.1016/s0031-6989(84)80094-6.

Aiello, A., Pepe, E., De Luca, L., Pizzolongo, F., Romano, R., 2022. Preliminary study on kinetics of pyroglutamic acid formation in fermented milk. Int. Dairy J. 126, 105233. https://doi.org/10.1016/j.idairyj.2021.105233.

van IJzendoorn, S.C.D., Derkinderen, P., 2019. The Intestinal Barrier in Parkinson's Disease: Current State of Knowledge. J. Park. Dis. 9, S323–S329. https://doi.org/10.3233/JPD-191707.

Vascellari, S., Palmas, V., Melis, M., Pisanu, S., Cusano, R., Uva, P., Perra, D., Madau, V., Sarchioto, M., Oppo, V., et al., 2020. Gut Microbiota and Metabolome Alterations Associated with Parkinson's Disease. mSystems 5, e00561–e620. https://doi.org/10.1128/mSystems.00561-20.

Henrich, M.T., Oertel, W.H., Surmeier, D.J., Geibl, F.F., 2023. Mitochondrial dysfunction in Parkinson's disease - a key disease hallmark with therapeutic potential. Mol. Neurodegener. 18, 83. https://doi.org/10.1186/s13024-023-00676-7.

Engelke, U.F.H., Zijlstra, F.S.M., Mochel, F., Valayannopoulos, V., Rabier, D., Kluijtmans, L.A.J., Perl, A., Verhoeven-Duif, N.M., de Lonlay, P., Wamelink, M.M.C., et al., 2010. Mitochondrial involvement and erythronic acid as a novel biomarker in transaldolase deficiency. Biochim. Biophys. Acta 1802, 1028–1035. https://doi.org/10.1016/j.bbadis.2010.06.007.

Pilarczyk-Zurek, M., Sitkiewicz, I., Koziel, J., 2022. The Clinical View on Streptococcus anginosus Group – Opportunistic Pathogens coming out of Hiding. Front. Microbiol. 13, 956677. https://doi.org/10.3389/fmicb.2022.956677.

Magdy Wasfy, R., Mbaye, B., Borentain, P., Tidjani Alou, M., Murillo Ruiz, M.L., Caputo, A., Andrieu, C., Armstrong, N., Million, M., Gerolami, R., 2023. Ethanol-Producing Enterocloster bolteae is Enriched in Chronic Hepatitis B-Associated Gut Dysbiosis: a Case-Control Culturomics Study. Microorganisms 11, 2437. https://doi.org/10.3390/microorganisms11102437.

Brisson-Noël, A., Delrieu, P., Samain, D., Courvalin, P., 1988. Inactivation of lincosaminide antibiotics in Staphylococcus. Identification of lincosaminide O-nucleotidyltransferases and comparison of the corresponding resistance genes. J. Biol. Chem. 263, 15880–15887.

Schönfeld, P., Wojtczak, L., 2016. Short- and medium-chain fatty acids in energy metabolism: the cellular perspective. J. Lipid Res. 57, 943–954. https://doi.org/10.1194/jlr.R067629.

Deleu, S., Arnauts, K., Deprez, L., Machiels, K., Ferrante, M., Huys, G.R.B., Thevelein, J. M., Raes, J., Vermeire, S., 2023. High Acetate Concentration Protects Intestinal Barrier and Exerts Anti-Inflammatory Effects in Organoid-Derived Epithelial Monolayer Cultures from patients with Ulcerative Colitis. Int. J. Mol. Sci. 24, 768. https://doi.org/10.3390/ijms24010768.

Chen, J.S., Faller, D.V., Spanjaard, R.A., 2003. Short-chain fatty acid inhibitors of histone deacetylases: promising anticancer therapeutics? Curr. Cancer Drug Targets 3, 219–236. https://doi.org/10.2174/1568009033481994.

Dalile, B., Van Oudenhove, L., Vervliet, B., Verbeke, K., 2019. The role of short-chain fatty acids in microbiota-gut-brain communication. Nat. Rev. Gastroenterol. Hepatol. 16, 461–478. https://doi.org/10.1038/s41575-019-0157-3.

Baert, F., Matthys, C., Maselyne, J., Van Poucke, C., Van Coillie, E., Bergmans, B., Vlaemynck, G., 2021. Parkinson's disease patients' short chain fatty acids production capacity after in vitro fecal fiber fermentation. NPJ Park. Dis. 7, 72. https://doi.org/10.1038/s41531-021-00215-5.

Verstraeten, S., Layec, S., Auger, S., Juste, C., Henry, C., Charif, S., Jaszczyszyn, Y., Sokol, H., Beney, L., Langella, P., et al., 2024. Faecalibacterium duncaniae A2-165 regulates the expression of butyrate synthesis, ferrous iron uptake, and stress-response genes based on acetate consumption. Sci. Rep. 14, 987. https://doi.org/10.1038/s41598-023-51059-3.

Zhou, Y., Xu, H., Xu, J., Guo, X., Zhao, H., Chen, Y., Zhou, Y., Nie, Y., 2021. F. prausnitzii and its supernatant increase SCFAs-producing bacteria to restore gut dysbiosis in TNBS-induced colitis. AMB Express 11, 33. https://doi.org/10.1186/s13568-021-01197-6.

Keegstra, J.M., Carrara, F., Stocker, R., 2022. The ecological roles of bacterial chemotaxis. Nat. Rev. Microbiol. 20, 491–504. https://doi.org/10.1038/s41579-022-00709-w.

Boktor, J.C., Sharon, G., Verhagen Metman, L.A., Hall, D.A., Engen, P.A., Zreloff, Z., Hakim, D.J., Bostick, J.W., Ousey, J., Lange, D., et al., 2023. Integrated Multi-Cohort Analysis of the Parkinson's Disease Gut Metagenome. Mov. Disord. off. J. Mov. Disord. Soc. 38, 399–409. https://doi.org/10.1002/mds.29300.

Guttenplan, S.B., Kearns, D.B., 2013. Regulation of flagellar motility during biofilm formation. FEMS Microbiol. Rev. 37, 849–871. https://doi.org/10.1111/1574-6976.12018.

Salemi, R.I., Cruz, A.K., Hershey, D.M., 2024. A flagellar accessory protein links chemotaxis to surface sensing. J. Bacteriol. 206, e0040424. https://doi.org/10.1128/jb.00404-24.

Giltner, C.L., Nguyen, Y., Burrows, L.L., 2012. Type IV pilin proteins: versatile molecular modules. Microbiol. Mol. Biol. Rev. MMBR 76, 740–772. https://doi.org/10.1128/MMBR.00035-12.

Persat, A., Inclan, Y.F., Engel, J.N., Stone, H.A., Gitai, Z., 2015. Type IV pili mechanochemically regulate virulence factors in Pseudomonas aeruginosa. PNAS 112, 7563–7568. https://doi.org/10.1073/pnas.1502025112.

Flemming, H.-C., Wuertz, S., 2019. Bacteria and archaea on Earth and their abundance in biofilms. Nat. Rev. Microbiol. 17, 247–260. https://doi.org/10.1038/s41579-019-0158-9.

Nie, S., Wang, J., Deng, Y., Ye, Z., Ge, Y., 2022. Inflammatory microbes and genes as potential biomarkers of Parkinson's disease. npj Biofilms Microbiomes 8, 101. https://doi.org/10.1038/s41522-022-00367-z.

Dunleavy, K.A., Rypstra, C.R., Busciglio, I., Eckert, D., Ryks, M., Omerdic, E., Chedid, V. G., Raffals, L.E., Camilleri, M., 2025. Intestinal Permeability In Vivo in patients with Inflammatory Bowel Disease: Comparison of active Disease and Remission. Inflamm. Bowel Dis. izaf043. https://doi.org/10.1093/ibd/izaf043.

Baldassano, S.N., Bassett, D.S., 2016. Topological distortion and reorganized modular structure of gut microbial co-occurrence networks in inflammatory bowel disease. Sci. Rep. 6, 26087. https://doi.org/10.1038/srep26087.

Colla, E., Coune, P., Liu, Y., Pletnikova, O., Troncoso, J.C., Iwatsubo, T., Schneider, B.L., Lee, M.K., 2012. Endoplasmic Reticulum stress is Important for the Manifestations of α-Synucleinopathy In Vivo. J. Neurosci. 32, 3306–3320. https://doi.org/10.1523/JNEUROSCI.5367-11.2012.

Mou, Z., Yuan, Y., Zhang, Z., Song, L., Chen, N.-H., 2020. Endoplasmic reticulum stress, an important factor in the development of Parkinson's disease. Toxicol. Lett. 324, 20–29. https://doi.org/10.1016/j.toxlet.2020.01.019.

Jiang, M., Yun, Q., Shi, F., Niu, G., Gao, Y., Xie, S., Yu, S., 2016. Downregulation of miR-384-5p attenuates rotenone-induced neurotoxicity in dopaminergic SH-SY5Y cells through inhibiting endoplasmic reticulum stress. Am. J. Physiol. Cell Physiol. 310. https://doi.org/10.1152/ajpcell.00226.2015.

Pazi, M.B., Belan, D.V., Komarova, E.Y., Ekimova, I.V., 2024. Intranasal Administration of GRP78 Protein (HSPA5) Confers Neuroprotection in a Lactacystin-Induced Rat Model of Parkinson's Disease. Int. J. Mol. Sci. 25, 3951. https://doi.org/10.3390/ijms25073951.

Gorbatyuk, M.S., Shabashvili, A., Chen, W., Meyers, C., Sullivan, L.F., Salganik, M., Lin, J.H., Lewin, A.S., Muzyczka, N., Gorbatyuk, O.S., 2012. Glucose regulated protein 78 diminishes α-synuclein neurotoxicity in a rat model of Parkinson disease. Mol. Ther. J. Am. Soc. Gene Ther. 20, 1327–1337. https://doi.org/10.1038/mt.2012.28.

Qu, Y., Li, J., Qin, Q., Wang, D., Zhao, J., An, K., Mao, Z., Min, Z., Xiong, Y., Li, J., et al., 2023. A systematic review and meta-analysis of inflammatory biomarkers in Parkinson's disease. Npj Park. Dis. 9, 18. https://doi.org/10.1038/s41531-023-00449-5.

Salganik, M., Sergeyev, V.G., Shinde, V., Meyers, C.A., Gorbatyuk, M.S., Lin, J.H., Zolotukhin, S., Gorbatyuk, O.S., 2015. The loss of Glucose Regulated Protein 78 (GRP78) during Normal Aging or from siRNA Knockdown Augments Human Alpha-Synuclein (α-syn) Toxicity to Rat Nigral Neurons. Neurobiol. Aging 36, 2213–2223. https://doi.org/10.1016/j.neurobiolaging.2015.02.018.

Enogieru, A.B., Omoruyi, S.I., Hiss, D.C., Ekpo, O.E., 2019. GRP78/BIP/HSPA5 as a Therapeutic Target in Models of Parkinson's Disease: a Mini Review. Adv. Pharmacol. Sci. 2019, 2706783. https://doi.org/10.1155/2019/2706783.

Recalde, D., Ostos, M.A., Badell, E., Garcia-Otin, A.-L., Pidoux, J., Castro, G., Zakin, M. M., Scott-Algara, D., 2004. Human apolipoprotein A-IV reduces secretion of proinflammatory cytokines and atherosclerotic effects of a chronic infection mimicked by lipopolysaccharide. Arterioscler. Thromb. Vasc. Biol. 24, 756–761. https://doi.org/10.1161/01.ATV.0000119353.03690.22.

Li, X., Liu, X., Zhang, Y., Cheng, C., Fan, J., Zhou, J., Garstka, M.A., Li, Z., 2021. Hepatoprotective effect of apolipoprotein A4 against carbon tetrachloride induced acute liver injury through mediating hepatic antioxidant and inflammation response in mice. Biochem. Biophys. Res. Commun. 534, 659–665. https://doi.org/10.1016/j.bbrc.2020.11.024.

Liu, X.-H., Zhou, J.-T., Yan, C., Cheng, C., Fan, J.-N., Xu, J., Zheng, Q., Bai, Q., Li, Z., Li, S., et al., 2022. Single-cell RNA sequencing reveals a novel inhibitory effect of ApoA4 on NAFL mediated by liver-specific subsets of myeloid cells. Front. Immunol. 13, 1038401. https://doi.org/10.3389/fimmu.2022.1038401.

Vowinkel, T., Mori, M., Krieglstein, C.F., Russell, J., Saijo, F., Bharwani, S., Turnage, R. H., Davidson, W.S., Tso, P., Granger, D.N., et al., 2004. Apolipoprotein A-IV inhibits experimental colitis. J. Clin. Invest. 114, 260–269. https://doi.org/10.1172/JCI21233.

Zhang, Y., He, J., Zhao, J., Xu, M., Lou, D., Tso, P., Li, Z., Li, X., 2017. Effect of ApoA4 on SERPINA3 mediated by nuclear receptors NR4A1 and NR1D1 in hepatocytes. Biochem. Biophys. Res. Commun. 487, 327–332. https://doi.org/10.1016/j.bbrc.2017.04.058.

Lin, Q., Cao, Y., Gao, J., 2015. Decreased expression of the APOA1–APOC3–APOA4 gene cluster is associated with risk of Alzheimer's disease. Drug Des. Devel. Ther. 9, 5421–5431. https://doi.org/10.2147/DDDT.S89279.

Cui, Y., Huang, M., He, Y., Zhang, S., Luo, Y., 2011. Genetic ablation of apolipoprotein A-IV accelerates Alzheimer's disease pathogenesis in a mouse model. Am. J. Pathol. 178, 1298–1308. https://doi.org/10.1016/j.ajpath.2010.11.057.

Kim, Y., Kim, J., Son, M., Lee, J., Yeo, I., Choi, K.Y., Kim, H., Kim, B.C., Lee, K.H., Kim, Y., 2022. Plasma protein biomarker model for screening Alzheimer disease using multiple reaction monitoring-mass spectrometry. Sci. Rep. 12, 1282. https://doi.org/10.1038/s41598-022-05384-8.

Tansey, M.G., Wallings, R.L., Houser, M.C., Herrick, M.K., Keating, C.E., Joers, V., 2022. Inflammation and immune dysfunction in Parkinson disease. Nat. Rev. Immunol. 22, 657–673. https://doi.org/10.1038/s41577-022-00684-6.

Yacoubian, T.A., Fang, Y.-H.-D., Gerstenecker, A., Amara, A., Stover, N., Ruffrage, L., Collette, C., Kennedy, R., Zhang, Y., Hong, H., et al., 2023. Brain and Systemic Inflammation in De Novo Parkinson's Disease. Mov. Disord. 38, 743–754. https://doi.org/10.1002/mds.29363.

Krishnan, R., Tsubery, H., Proschitsky, M.Y., Asp, E., Lulu, M., Gilead, S., Gartner, M., Waltho, J.P., Davis, P.J., Hounslow, A.M., et al., 2014. A bacteriophage capsid protein provides a general amyloid interaction motif (GAIM) that binds and remodels misfolded protein assemblies. J. Mol. Biol. 426, 2500–2519. https://doi.org/10.1016/j.jmb.2014.04.015.

Dimant, H., Sharon, N., Solomon, B., 2009. Modulation effect of filamentous phage on alpha-synuclein aggregation. Biochem. Biophys. Res. Commun. 383, 491–496. https://doi.org/10.1016/j.bbrc.2009.04.048.

Dimant, H., Solomon, B., 2010. Filamentous phages reduce alpha-synuclein oligomerization in the membrane fraction of SH-SY5Y cells. Neurodegener Dis 7, 203–205. https://doi.org/10.1159/000295664.

Arcos, M., Olivera, E.R., Arias, S., Naharro, G., Luengo, J.M., 2010. The 3,4-dihydroxyphenylacetic acid catabolon, a catabolic unit for degradation of biogenic amines tyramine and dopamine in Pseudomonas putida U. Environ. Microbiol. 12, 1684–1704. https://doi.org/10.1111/j.1462-2920.2010.02233.x.

Sandler, M., Karoum, F., Ruthven, C.R., Calne, D.B., 1969. m-Hydroxyphenylacetic acid formation from L-dopa in man: suppression by neomycin. Science 166, 1417–1418. https://doi.org/10.1126/science.166.3911.1417.

Liu, Z., Xi, R., Zhang, Z., Li, W., Liu, Y., Jin, F., Wang, X., 2014. 4-hydroxyphenylacetic acid attenuated inflammation and edema via suppressing HIF-1α in seawater aspiration-induced lung injury in rats. Int. J. Mol. Sci. 15, 12861–12884. https://doi.org/10.3390/ijms150712861.

Zhao, H., Jiang, Z., Chang, X., Xue, H., Yahefu, W., Zhang, X., 2018. 4-Hydroxyphenylacetic Acid Prevents Acute APAP-Induced Liver Injury by increasing phase II and Antioxidant Enzymes in mice. Front. Pharmacol. 9, 653. https://doi.org/10.3389/fphar.2018.00653.

An, S., Yao, Y., Wu, J., Hu, H., Wu, J., Sun, M., Li, J., Zhang, Y., Li, L., Qiu, W., et al., 2024. Gut-derived 4-hydroxyphenylacetic acid attenuates sepsis-induced acute kidney injury by upregulating ARC to inhibit necroptosis. Biochim. Biophys. Acta Mol. basis Dis. 1870, 166876. https://doi.org/10.1016/j.bbadis.2023.166876.

Xiang, Y., Zhang, C., Wang, J., Cheng, Y., Wang, K., Wang, L., Tong, Y., Yan, D., 2024. Role of blood metabolites in mediating the effect of gut microbiome on the mutated-RAS/BRAF metastatic colorectal cancer-specific survival. Int. J. Colorectal Dis. 39, 116. https://doi.org/10.1007/s00384-024-04686-9.